Neutrino mass tension or suppressed growth rate of matter perturbations?

William Giarè,[1,*] Olga Mena,[2,†] Enrico Specogna,[1,‡] and Eleonora Di Valentino[1,§]
[1]*School of Mathematical and Physical Sciences, University of Sheffield, Hounsfield Road, Sheffield S3 7RH, United Kingdom*
[2]*Instituto de Física Corpuscular (IFIC), University of Valencia-CSIC, Parc Científic UV, c/ Catedrático José Beltrán 2, E-46980 Paterna, Spain*

(Received 21 July 2025; accepted 29 October 2025; published 14 November 2025)

Assuming a minimal Λ cold dark matter (ΛCDM) cosmology with three massive neutrinos, the joint analysis of Planck cosmic microwave background data, DESI baryon acoustic oscillations, and distance moduli measurements of type Ia supernovae from the Pantheon + sample sets an upper bound on the total neutrino mass, $\sum m_\nu \lesssim 0.06$–0.07 eV, that lies barely above the lower limit from oscillation experiments. These constraints are mainly driven by mild differences in the inferred values of the matter density parameter across different probes that can be alleviated by introducing additional background-level degrees of freedom (e.g., by dynamical dark energy models). However, in this work, we explore an alternative possibility. Since both $\Omega_{\rm m}$ and massive neutrinos critically influence the growth of cosmic structures, we test whether the neutrino mass tension may originate from the way matter clusters, rather than from a breakdown of the ΛCDM expansion history. To this end, we introduce the growth index γ, which characterizes the rate at which matter perturbations grow. Deviations from the standard ΛCDM value ($\gamma \simeq 0.55$) can capture a broad class of models, including nonminimal dark sector physics and modified gravity. We show that allowing γ to vary significantly relaxes the neutrino mass bounds to $\sum m_\nu \lesssim 0.13$–0.2 eV, removing any tension with terrestrial constraints without altering the inferred value of $\Omega_{\rm m}$. However, this comes at the cost of departing from standard growth predictions: to have $\sum m_\nu \gtrsim 0.06$ eV, one needs $\gamma > 0.55$, and we find a consistent preference for $\gamma > 0.55$ at the level of $\sim 2\sigma$. This preference increases to ~ 2.5–3σ when a physically motivated prior $\sum m_\nu \geq 0.06$ eV from oscillation experiments is imposed.

DOI: 10.1103/njfc-pd1w

I. INTRODUCTION

What began as Pauli's desperate remedy to preserve energy conservation in beta decay—the postulation of light, electrically neutral, and almost undetectable particles, soon to be called neutrinos—has since grown into one of the most remarkable success stories in modern physics. Despite Pauli's own skepticism about the testability of his hypothesis, not only have three distinct families of neutrinos been experimentally confirmed, but neutrino oscillation experiments have also precisely measured two independent mass-squared differences: $|\Delta m^2_{31}| \equiv |m^2_3 - m^2_1| \simeq 2.5 \times 10^{-3}\ \text{eV}^2$ and $\Delta m^2_{21} \equiv m^2_2 - m^2_1 \simeq 7.5 \times 10^{-5}\ \text{eV}^2$ [1–3].

On the one hand, these measurements imply that at least two neutrino species have nonzero mass, providing concrete evidence for physics beyond the Standard Model, where neutrinos are originally treated as massless particles. Explaining neutrino masses—either through the effective dimension-five Weinberg operator [4], which induces small Majorana masses by violating lepton number, or via more elaborate seesaw mechanisms that introduce heavy right-handed neutrinos [5–8]—remains an open challenge that attracts significant research interest.

On the other hand, since the sign of Δm^2_{31} remains unknown, two possible mass orderings are still allowed: the *normal ordering* (NO) $\Delta m^2_{31} > 0$ and the *inverted ordering* (IO) $\Delta m^2_{31} < 0$. In both orderings, assuming the lightest neutrino mass is zero, neutrino oscillation experiments provide a lower limit on the total neutrino mass, $\sum m_\nu \equiv m_1 + m_2 + m_3$. This reads $\sum m_\nu > 0.06$ eV for the NO and $\sum m_\nu > 0.1$ eV for the IO [2].

*Contact author: w.giare@sheffield.ac.uk
†Contact author: omena@ific.uv.es
‡Contact author: especogna1@sheffield.ac.uk
§Contact author: e.divalentino@sheffield.ac.uk

Given their intrinsic importance,[1] determining the neutrino mass ordering and precisely measuring the total neutrino mass $\sum m_\nu$ remain key objectives of neutrino physics. To this end, a number of ongoing and future neutrino oscillation experiments have been designed to resolve the mass ordering while simultaneously improving constraints on $\sum m_\nu$ [11–15]; see also Ref. [16]. Complementing these efforts, direct searches such as the KATRIN experiment provide competitive upper bounds on the total neutrino mass, currently $\sum m_\nu < 1.35$ eV [17].

On the cosmological side, in the simplest scenario—that is, within the standard Λ cold dark matter (ΛCDM) model and three degenerate neutrino states—the DESI Collaboration has recently reported that when DESI-2025 baryon acoustic oscillation (BAO) measurements are combined with Planck-PR4 cosmic microwave background (CMB) likelihoods, the cosmological upper limit on the total neutrino mass reads $\sum m_\nu \lesssim 0.064$ eV [18] at 95% confidence level (CL). This is worryingly close to the lower limits set by oscillation experiments within the NO and in strong tension with the IO. Furthermore, when extending the analysis to other sources of cosmological and astrophysical data, the cosmological bound on the total neutrino mass can be pushed even below the minimum scale predicted by terrestrial oscillation experiments, i.e., around $\sum m_\nu \lesssim 0.05$ eV [19], leading to an overall tension between oscillation results and cosmological observations [20].[2] Although part of this tension may reflect differences or inconsistencies across datasets, an even more striking feature emerges when the well-motivated physical prior $\sum m_\nu > 0$ (used in the DESI analyses) is relaxed, and the unphysical region $\sum m_\nu < 0$ is allowed. In this case, negative neutrino masses are found to be favored by the data, as reported by several independent groups [25–29].

It now appears well established that, within the minimal ΛCDM framework, the extremely small values inferred for the total neutrino mass largely originate from a mismatch in the preferred value of Ω_m [18,25,30–33]. In particular, BAO distance measurements from DESI favor a lower matter density, which lies in moderate $(2-3\sigma)$ tension with values inferred from CMB observations. This tension often manifests as a preference for unnaturally small values of $\sum m_\nu$.[3]

Interestingly, when considering extended cosmological scenarios—most notably those allowing for dynamical dark energy—the discrepancy is somewhat alleviated. As originally shown by the DESI Collaboration [46–48] and subsequently corroborated by multiple reanalyses [39,43,45,49–94], adopting a Chevallier Polarski Linder (CPL) parametrization [95,96], in which the dark energy equation of state varies linearly with the expansion history of the Universe, leads to a significantly improved consistency between DESI BAO and Planck CMB data. In this extended scenario, a preference for dynamical dark energy emerges at the $2.8-4.2\sigma$ level, depending on the specific dataset combination. At the same time, the neutrino mass bounds are relaxed up to $\sum m_\nu < 0.16$ eV, restoring agreement with oscillation experiments [3,47].

Given the mounting evidence for dynamical dark energy and its resilience across diverse independent probes, the predominant—though far from unanimous[4]—narrative surrounding the neutrino mass problem is that the unphysically small cosmological upper limits on $\sum m_\nu$ may themselves reflect the inability of the minimal ΛCDM model to accurately describe the late-time expansion of the Universe. In other terms, within the minimal ΛCDM model, the late-time behavior of $H(z)$ is tightly governed by only two parameters: the present-day Hubble constant H_0 and the matter density parameter Ω_m. Stringent constraints from DESI BAO data on the transverse comoving

[1]For example, neutrinoless double beta decay searches, which investigate the possible Majorana nature of neutrinos (namely, whether neutrinos are their own antiparticles), depend crucially on both the absolute neutrino mass scale and their hierarchical ordering [9,10].

[2]Note that pre-2024 cosmological constraints on $\sum m_\nu$ ranged from the conservative 95% CL limit $\sum m_\nu \lesssim 0.2$ eV quoted by the Planck Collaboration in Ref. [21] all the way up to the tightest bounds $\sum m_\nu \lesssim 0.09$ eV [22–24] resulting from joint analyses of Planck PR3 CMB data and late-time expansion history probes in the form of distance measurements from BAO and type Ia supernovae (SNIa). While the most constraining results placed the IO under some tension, the exact preference for the NO over the IO (and more broadly, the tightest limits themselves) varied significantly depending on the number of underlying assumptions and datasets involved in the different analyses. Therefore, before DESI BAO data, discussions surrounding preferences for specific orderings and tensions in neutrino cosmology were somewhat academic in nature.

[3]It is worth noting that, assuming a ΛCDM cosmology, this tension must necessarily originate from systematic effects responsible for the discrepancies among datasets. In addition to the possibility of undetected systematics in DESI BAO measurements [27,34–40], another relevant factor is the prominent role played by CMB data [41]. Even before the release of the DESI results, some of us had already shown that temperature and polarization measurements particularly at large scales can be affected by anomalies that influence constraints on parameters tightly correlated with $\sum m_\nu$, such as τ and $A_{\rm lens}$ [42]. Following the DESI results, several independent analyses confirmed that relaxing the constraints from large-scale E-mode polarization and allowing $A_{\rm lens}$ to vary can significantly weaken the bounds quoted earlier [3,32,33,43–45].

[4]With no intention to underplay the robustness and intrinsic interest of the hints for dynamical dark energy that emerged after DESI, we note that this interpretation is not without caveats. Both the DESI result and the preference for dynamical dark energy have been the subject of debate and several reinterpretations [27,30,34–36,38,40,41,49,68,97,98]. Furthermore, while dynamical dark energy appears to be well supported by observations, it is unable to resolve or alleviate other major tensions in cosmology, such as the Hubble tension [99–113], leaving room for the exploration of more elaborate scenarios potentially capable of systematically accounting for all these problems simultaneously; see, e.g., Refs. [56,78,114–117].

distance $D_M(z)$, the Hubble parameter $H(z)$, and their combination $D_V(z)$ (all expressed relative to the sound horizon at the drag epoch r_d) translate directly into stringent bounds on Ω_m, driving the mismatch between cosmological upper limits and terrestrial lower limits on the total neutrino mass. Conversely, an evolving dark energy equation of state introduces additional freedom into $H(z)$, allowing more flexibility in fitting BAO measurements at different redshift while accommodating values of Ω_m that are in line with CMB-derived estimates. As a result, the differences in the inferred value of the matter density, combined with the enlarged parameter space, weaken the degeneracy between Ω_m and $\sum m_\nu$, relaxing the upper bounds on the neutrino mass.[5] In this sense, one could argue that dynamical dark energy can be regarded as a solution that operates almost entirely at the level of *background* dynamics, leaving minimal effects at the level of perturbations in the CMB spectra.

Although this interpretation has gained significant traction, in this work, we wish to propose and explore a complementary perspective on the neutrino mass discrepancy by shifting the focus from the expansion history to the growth of cosmic structures. The key observation motivating this shift is that both Ω_m and $\sum m_\nu$ not only affect the background expansion but also critically influence the growth of cosmic structures, driving gravitational clustering of overdensities and suppressing structure formation at small scales, respectively. Consequently, a mismatch between cosmological and terrestrial bounds on the total neutrino mass may point to new physics impacting not only the background expansion but also the dynamics of the growth rate of matter perturbations over time, and structure formation more broadly—either alongside or instead of modifications to the expansion history.

To test this possibility, we consider a nonstandard growth of structure by introducing a free growth index parameter, γ [151,152]. This index effectively captures the physics of structure growth across a wide range of alternative scenarios, from dark energy models to beyond-Einstein gravity. Crucially, γ does not alter the background expansion. Instead, it directly impacts observables sensitive to matter perturbations, such as the CMB spectra and the matter power spectrum. This makes it possible to disentangle different models based on their perturbation-level effects, even when their expansion histories are identical. In this sense, it offers a clean framework to test whether new physics affecting the growth of structure can provide an alternative and complementary route to reconcile cosmological and terrestrial bounds on the neutrino mass. To this end, we perform a comprehensive analysis combining the latest DESI BAO data, Planck CMB likelihoods, and type Ia supernova distance moduli measurements, explicitly allowing for departures from ΛCDM at the *perturbation* level while keeping the background fixed to the baseline model.

The structure of the manuscript is as follows. We start in Sec. II by describing the linear growth factor and the growth index parameter, illustrating the degeneracy between the former and the neutrino mass. Section III presents the different datasets employed in the analyses and the methodology followed to derive the results presented in Sec. IV. We draw our conclusions in Sec. V.

II. GROWTH INDEX AND NEUTRINOS

As emphasized in the Introduction, our goal is to assess whether the unphysically tight bounds on the total neutrino mass, arising from the mild tension between the values of Ω_m preferred by geometric probes like BAO and those inferred from perturbation-sensitive observables such as the CMB in ΛCDM, may be driven, at least in part, by the assumption of standard structure growth, without necessarily indicating a failure of the standard background expansion, as in dynamical dark energy models. In this regard, many well-motivated extensions of the standard cosmological model predict a background evolution virtually identical to that of ΛCDM. Consequently, these models exhibit degeneracy in $\Omega_m(a)$ and cannot be distinguished based on background-level predictions alone. This happens, for instance, in those ΛCDM extensions where the effective equation of state of the accelerating component in the Hubble equation (whether this is dark energy or a modification of gravity) is free to vary slightly around -1 [153]. Similarly, in the DGP model [154], one can reproduce the same expansion history predicted by fixing $w_0 = -0.78$ and $w_a = 0.32$ in the CPL parametrization [151], making it hard to distinguish different models by means of background quantities only. However, such models can still produce distinct signatures in structure formation. If the actual growth of structures deviates from the ΛCDM expectation, these deviations could partially mimic or offset the effects usually attributed to massive neutrinos. Hence, the evolution of matter perturbations offers a powerful probe of alternative scenarios, ranging from modified gravity theories to nonminimal dark sector physics.

The growth of density perturbations can be studied using the perturbed equations of motion derived from the underlying gravitational theory. In the subhorizon, linear regime, the physical interpretation is straightforward: the growth is driven by a source term proportional to the amount of matter that can cluster, and suppressed by a friction term—often referred to as Hubble drag—associated with the expansion of the Universe [155,156].

A key observable in this regime is the growth rate of structure, defined as

[5]We note that yet another key assumption underlying cosmological limits on the total neutrino mass is the standard neutrino physics. Many alternative models of new physics in the neutrino sector have been proposed and remain viable and actively explored alternatives, often leading to weaker cosmological bounds on $\sum m_\nu$. Without any claim of completeness, see, e.g., Refs. [25,118–150].

$$f = \frac{d \ln \delta_{\rm m}}{d \ln a} = \frac{\delta'_{\rm m}}{\delta_{\rm m}} a, \tag{1}$$

where $\delta_{\rm m}$ is the matter density contrast and $'$ denotes the derivative with respect to the scale factor. The growth rate captures how efficiently matter overdensities grow over time, from their primordial seeds to the observed large-scale structure.

A commonly used approach to capture deviations from standard structure formation history is to introduce the so-called growth index γ [151,157], defined as the exponent that yields a power-law solution to the growth rate equation in terms of the matter density parameter,

$$f(a) \simeq \Omega_m(a)^\gamma \simeq \left[\frac{\Omega_{\rm m} a^{-3}}{\Omega_{\rm de}(a) + \Omega_{\rm m} a^{-3}}\right]^\gamma. \tag{2}$$

Note that, in this expression, $\Omega_m(a)$ denotes the matter density fraction at scale factor a.

Although γ can, in general, acquire a time and/or scale dependence according to the underlying theory of gravity or dark energy, in many relevant cases, it can be accurately approximated as a constant. For a dark energy fluid with constant equation of state w, one finds $\gamma \simeq 3(w-1)/(6w-5)$ [152], which gives the canonical value $\gamma = 6/11 \simeq 0.55$ in the ΛCDM case ($w = -1$) [151]. In many alternative scenarios, however, γ can differ substantially. Just to mention a few concrete examples: in DGP braneworld gravity, one finds $\gamma \approx 0.68$, with less than 2% variation when treated as constant [151,152], while in $f(R)$ gravity models with mild scale dependence, $\gamma \approx 0.4$ [158], though a significant time dependence may still arise, with present-day slopes as large as $\gamma' \simeq -0.2$ [159].

Overall, the growth index plays a central role in linking theory to observations concerning the clustering of matter perturbations. Specifically, in linear perturbation theory, the evolution of matter inhomogeneities is governed by the linear growth function, defined as $D(a) \equiv \delta_{\rm m}(a)/\delta_{\rm m}(a_0)$, and satisfying $f(a) \equiv d \ln D(a)/d \ln a$. Assuming the parametrization in Eq. (2) with constant γ, we obtain [160,161]

$$D(\gamma, a) = \exp\left[-\int_a^1 \frac{\Omega_{\rm m}(a)^\gamma}{a} da\right], \tag{3}$$

where the growth function is normalized such that $D(\gamma, a = 1) = 1$ for all values of γ. This introduces an important subtlety that will be crucial for interpreting the following results in the context of massive neutrino cosmologies. Namely, models predicting a larger growth index, i.e., $\gamma > 0.55$, imply a *slower* growth rate at any given epoch. Indeed, since $\Omega_{\rm m}(a) < 1$ by construction, Eq. (2) implies $f(\gamma > 0.55, a) < f(\gamma = 0.55, a)$, corresponding to a lower formation rate. However, due to the normalization $D(a = 1) = 1$, a slower growth rate today implies that the linear growth function must have been *larger* in the past to reach the same amplitude at present. In other words, we find that $D(\gamma > 0.55, a) > D(\gamma = 0.55, a)$ for $a < 1$. As a result, models with larger γ predict an enhanced growth function in the past, despite a systematically reduced growth rate throughout cosmic history.

Keeping this result in mind, when it comes to massive neutrinos, many important observations are in order to clarify their impact on structure formation and their connection with the growth index γ.

First and foremost, once neutrinos become non-relativistic particles, they contribute to the total nonrelativistic matter density—a contribution that depends ultimately on the value of the total neutrino mass. It is therefore unsurprising that different values of $\sum m_\nu$ would inherently affect the theoretical value of the growth index γ, even within the standard ΛCDM framework. An analytical expression for the growth rate f in the presence of massive neutrinos was derived in Ref. [162]. However, we have numerically confirmed that, even for total neutrino masses well above the current observational limits, the theoretical variations in γ remain negligible compared to the uncertainties in its inferred value. Consequently, having established that the theoretical impact of treating neutrinos as massive particles on γ is effectively negligible for the purpose of this study, we will use $\gamma = 0.55$ as our reference value in the following analysis to test deviations from the ΛCDM model.

A second, more subtle but important point—partially noted in the Introduction—is that both massive neutrinos and deviations from the canonical growth index value impact cosmological observables related to perturbations (such as the CMB angular power spectra and the matter power spectrum) in distinct yet qualitatively similar ways.

Massive neutrinos affect the angular power spectra of CMB temperature and polarization anisotropies through several mechanisms: by contributing to the late-time non-relativistic energy density, they alter the angular scale relation at the last scattering surface and modify the late integrated Sachs-Wolfe (ISW) effect. Moreover, the exact value of $\sum m_\nu$ influences the neutrino transition to the nonrelativistic regime by changing their pressure-to-density ratio, inducing metric fluctuations visible in the early ISW effect. Most significantly, massive neutrinos suppress the growth of structure, reducing the amplitude of the matter power spectrum. This suppression also affects the weak lensing of the CMB, damping power on small angular scales.[6] The overall impact on the CMB power spectra includes a reduction in the amplitude of the first acoustic peak (mainly due to the ISW effect) and also a shifting of higher acoustic peaks toward lower multipoles. These effects are illustrated in the left panel of Fig. 1, which compares two reference total neutrino mass values: $\sum m_\nu = 0.06$ eV (the minimum mass consistent with oscillation experiments and commonly assumed in ΛCDM) and an unphysically large

[6]For constraints on the neutrino mass based on CMB lensing or damping tail effects, see Refs. [163,164].

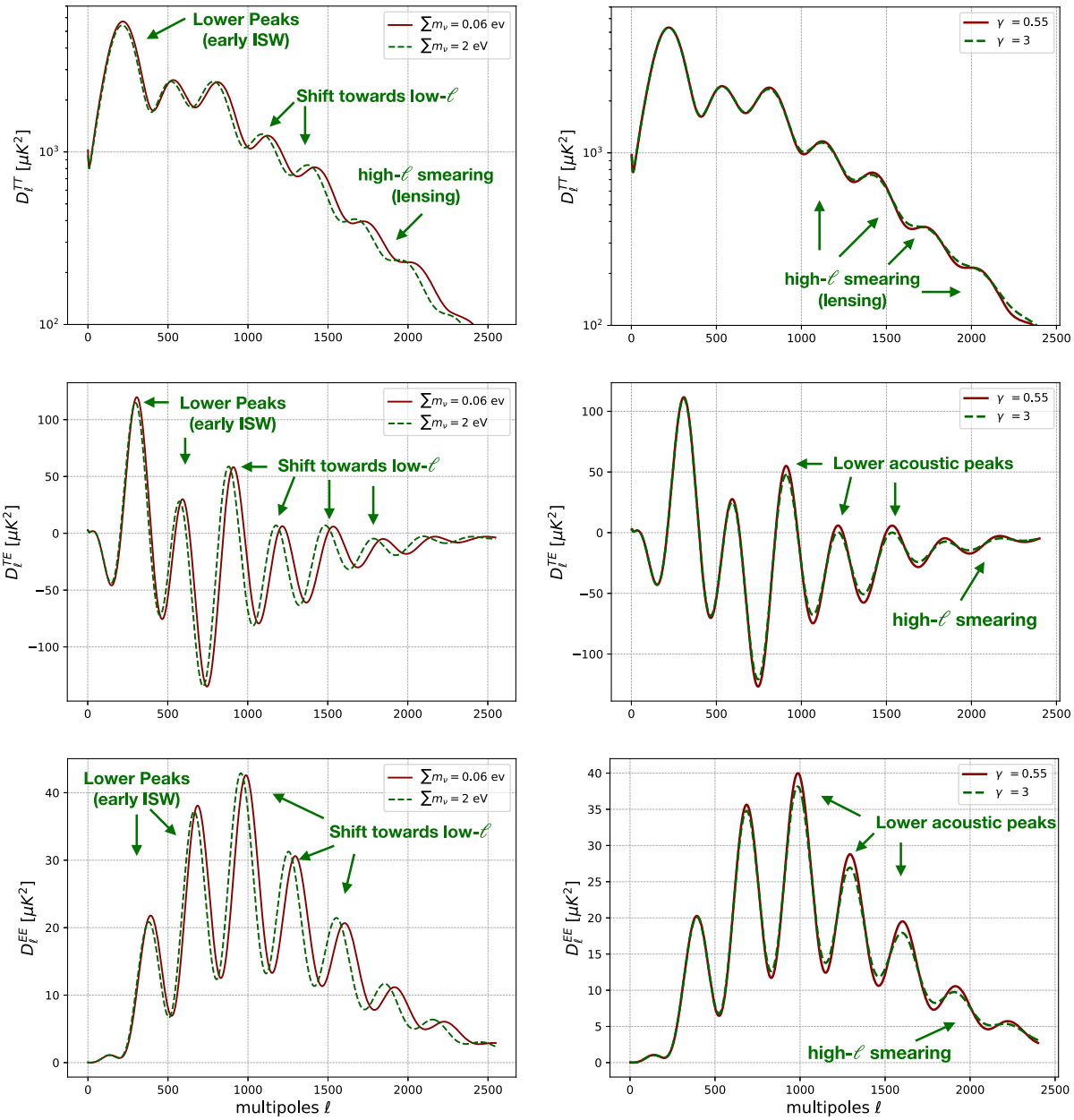

FIG. 1. CMB temperature, polarization and cross-correlation power spectra for different values of the total neutrino mass (left panels), and for different values of the growth index γ (right panels), see text for details.

mass of $\sum m_\nu = 2$ eV, chosen to clearly highlight the effects described above.

Similarly, noncanonical values of the growth index γ directly modify the rate at which matter perturbations grow over time, affecting the amplitude and evolution of matter density fluctuations, which in turn influence secondary anisotropies in the CMB through gravitational lensing. Roughly speaking, since the lensing potential is highly sensitive to the distribution and amplitude of matter fluctuations along the line of sight, a growth index different from the canonical $\gamma \approx 0.55$ will alter the clustering strength of matter, changing the gravitational potential wells that CMB photons traverse on their journey toward us. This modification of the gravitational potentials affects the lensing of the CMB by smoothing the acoustic peaks in the temperature and polarization power spectra. This smoothing occurs because lensing deflects the paths of CMB photons, mixing power between different multipoles and reducing the sharpness of the acoustic peaks. As shown in the right panel of Fig. 1, increasingly large values of $\gamma > 0.55$ produce more pronounced smoothing at small angular scales (high multipoles)—exactly where the temperature anisotropy spectrum becomes approximately linearly dependent on the lensing power spectrum [165]. This effect can be easily compensated by increasing the neutrino mass, since neutrinos, which are hot dark matter particles,

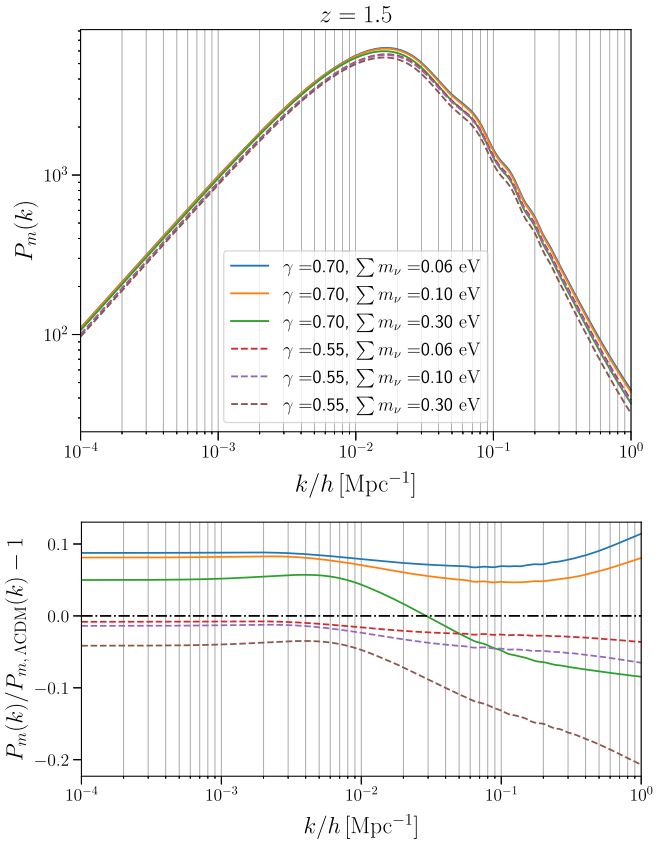

FIG. 2. Matter power spectrum at redshift $z = 1.5$ for a standard growth scenario ($\gamma = 0.55$, dashed lines) and a modified one with $\gamma = 0.7$ (solid lines). The different colors depict different values of the total neutrino mass, namely $\sum m_\nu = 0.06$, 0.1, and 0.3 eV. In the bottom panel, we show the ratios of the power spectra for the different parameter cases relative to the ΛCDM model.

reduce CMB lensing as they suppress clustering at small scales [166,167], leading to a less pronounced smoothing at low multipoles. Consequently, a large, positive degeneracy is expected among these two parameters, as we will precisely see in the results of our numerical analyses when both γ and $\sum m_\nu$ are free parameters of the model.

Another way to understand the similar effects of γ and $\sum m_\nu$ is by examining their impact on the matter power spectrum. This key complementary observable (which is ultimately linked to the CMB power spectra, especially at high multipoles) provides a direct way to quantify how deviations in γ and the total neutrino mass impact the amplitude and shape of matter fluctuations. Figure 2 depicts the matter power spectrum at $z = 1.5$ for the standard structure formation scenario with $\gamma = 0.55$ and a modified one with $\gamma = 0.7$. Three different possible values for $\sum m_\nu$ have been considered, namely the smallest total neutrino mass consistent with particle physics experiments ($\sum m_\nu = 0.06$ eV) and two other possible cases, $\sum m_\nu = 0.1$ eV and $\sum m_\nu = 0.3$ eV. As expected, larger neutrino masses suppress the matter power spectrum. Neutrinos are hot dark matter relics with very large velocity dispersions, suppressing the growth of structure at scales smaller than their free-streaming scale when they turn nonrelativistic. The amount of suppression depends on the precise value of the total neutrino mass.

On the other hand, in cosmologies with a nonstandard growth rate, the linear matter power spectrum can be expressed as [160,161]

$$P_{\mathrm{m}}(\gamma, k, a) = P_{\mathrm{m}}^{\Lambda\mathrm{CDM}}(k, a = 1) D^2(\gamma, a), \tag{4}$$

where $P_{\mathrm{m}}^{\Lambda\mathrm{CDM}}(k, a = 1)$ is the fiducial linear matter power spectrum evaluated today, while $D(\gamma, a)$ is the growth function defined in Eq. (3). As previously pointed out, a larger value of the growth index γ suppresses the growth rate f, while enhancing the growth function $D(\gamma, a)$ at earlier times. According to Eq. (4), this translates into an enhanced matter power spectrum in the past (as seen in Fig. 2 at $z = 1.5$). As a result, a positive degeneracy between $\sum m_\nu$ and γ is expected: the suppression of structure formation due to larger neutrino masses can be partially compensated by a larger value of γ, which boosts the amplitude of $D(\gamma, a)$ and hence of the matter power spectrum. This is the case illustrated in Fig. 2, where the matter power spectrum obtained for $\sum m_\nu = 0.1$ eV and $\gamma = 0.55$, is nearly indistinguishable from the case of $\sum m_\nu = 0.3$ eV and $\gamma = 0.7$, at least for $k/h > 0.1$ Mpc^{-1}. It is therefore expected that modified growth scenarios with $\gamma > 0.55$ can easily accommodate larger neutrino masses, and this very interesting possibility should be carefully analyzed with the most recent cosmological observations, as we shall present in the following sections.

III. METHODOLOGY AND DATASETS

The considerations outlined in Sec. II motivate us to analyze extensions of the ΛCDM parameter space—hereafter referred to as λ—by including γ and $\sum m_\nu$ as additional free parameters.[7] In particular, we consider the following extended parameter space combinations:

(i) $\lambda \cup \{\sum m_\nu\}$,
(ii) $\lambda \cup \{\gamma\}$, and
(iii) $\lambda \cup \{\sum m_\nu, \gamma\}$.

The cosmology calculations have been performed with a patched version of the Boltzmann solver CAMB [168,169], specifically adapted for the γ parametrization of modified gravity: CAMB_GammaPrime_Growth [160]. We stress that, while γ can, in general, be time-dependent, in this paper, we take it to be constant at all redshifts.

[7]Note that λ includes the six standard model parameters, namely: the matter densities of baryons ($\Omega_{\mathrm{b}}h^2$) and dark matter ($\Omega_{\mathrm{c}}h^2$), the optical depth to reionization (τ), the amplitude (A_s) and spectral index (n_s) of the primordial scalar fluctuations, and the angular size of the sound horizon at last scattering (θ_{MC}).

TABLE I. Flat priors adopted for the parameters presented in Sec. III. The label "NO" denotes an additional prior restriction on $\sum m_\nu$, accounting for the normal neutrino ordering constraints from particle physics experiments [2].

Parameter	Prior
$\Omega_b h^2$	[0.005, 0.1]
$\Omega_c h^2$	[0.001, 0.99]
τ	[0.01, 0.8]
n_s	[0.8, 1.2]
$\log(10^{10} A_s)$	[1.61, 3.91]
$100\theta_{\rm MC}$	[0.5, 10]
$\sum m_\nu$ [eV]	[0, 5]
$\sum m_\nu$ [eV] (NO)	[0.06, 5]
γ	[0, 1]

To efficiently explore the extended parameter spaces, we perform Markov chain Monte Carlo (MCMC) analyses using the Cobaya sampler [170], varying the cosmological parameters within the flat priors listed in Table I. Note that, as explained in more detail in the next section, for the total neutrino mass we consider two relevant cases: one in which we impose a lower prior limit $\sum m_\nu > 0.06$ eV, based on oscillation experiment results assuming the NO, and another in which this lower limit is relaxed to $\sum m_\nu > 0$ eV. We ensure that all produced chains satisfy the Gelman Rubin convergence criterion, requiring a convergence threshold of $R < 0.01$. These chains are then analyzed using the GetDist package [171] to derive constraints on the parameter space and generate the plots presented in Sec. IV.

The dataset employed in our analysis includes two different combinations of likelihood releases for the CMB spectra measured by the Planck satellite. In particular,

(i) *Plik*: This includes the Planck-PR3 likelihood PLIK [172] for the temperature (TT), polarization (EE), and temperature polarization cross-correlation (TE) spectra at $\ell > 30$, the SIMALL likelihood [21] for E-mode polarization measurements at $\ell < 30$, and the Commander likelihood [173] for temperature anisotropies at $\ell < 30$. The PLIK lensing likelihood [174] is also included in this combination.

(ii) *Camspec*: This includes the Camspec [175] likelihood for the TT, TE, and EE spectra at $\ell > 30$, based on the Planck-PR4 NPIPE CMB maps [176], always in combination with the SIMALL likelihood [21] for E-mode polarization and the Commander likelihood [173] for temperature anisotropies at $\ell < 30$. In this combination, for CMB lensing, we use the Planck-PR4 NPIPE lensing likelihood [176,177].

Note that we consider these two independent combinations of likelihoods for very important reasons: over the years, several mild anomalies have been identified in the Planck-PR3 data, many of which can alter the constraints on the parameters of interest in this study. The most significant example is the excess smoothing of acoustic peaks observed in the Planck-PR3 spectra, which appears to be reduced in the PR4 likelihoods based on the NPIPE maps.[8] Several groups have highlighted that these differences in excess smoothing between the PR3 and PR4 high-multipole likelihoods can significantly impact constraints on the total neutrino mass [3,20,27,182–186]. Similarly, as first shown by some of us in Ref. [187] and subsequently confirmed by the DESI Collaboration itself [188,189], the overall differences in smoothing between the Planck-PR3 and Planck-PR4 spectra also have important consequences for constraints on the growth index γ. Depending on which high-multipole CMB likelihood is used, CMB constraints on γ can vary significantly, resulting in either better or worse agreement with the baseline ΛCDM prediction [187]. Given the significant impact of choosing either the Planck-PR3 or Planck-PR4 likelihoods on the constraints of both parameters of interest, it is not only important, but in fact essential, to consider both combinations in order to draw reliable conclusions.

In addition to the CMB data outlined above, we consider geometrical probes of the late Universe in the form of precise constraints on the transverse comoving distance, the Hubble rate, and their combination (all relative to the sound horizon at the drag epoch), derived from BAO data and distance modulus measurements from SNIa. In particular, we consider

(i) *DESI*: This includes the isotropic and anisotropic BAO measurements from the second data release by the DESI Collaboration, based on observations of over 14 million extragalactic objects such as galaxies and quasars [190], as well as Lyman-α tracers [191]. These measurements are summarized in Table IV of Ref. [47].

(ii) *PP*: These are the distance moduli obtained from observations of 1550 SNIa up to $z = 2.26$ in the Pantheon + sample, without the inclusion of Cepheid host distances [192].

In closing, we would like to spend a few words on the choice of the SNIa sample adopted in this analysis. At present, three independent compilations are available—Pantheon+ [192], DESy5 [193–195], and Union3 [196]—each constructed from different observational datasets and calibration strategies. Including all of them would considerably inflate the number of combinations under

[8]This effect can be accurately quantified through the phenomenological parameter $A_{\rm lens}$ [178], which captures the amplitude of the lensing power spectrum inferred from the smoothing of acoustic peaks in the temperature and polarization spectra. Analyses based on the Plik PR3 spectra suggest that $A_{\rm lens}$ deviates from the expected baseline value ($A_{\rm lens} = 1$) at the level of about 2.8σ [21,179–181]. In contrast, when using the temperature and polarization PR4 spectra from Camspec, the preference for $A_{\rm lens} > 1$ is reduced to below 1.7σ [175], even if this comes at the cost of a moderate internal disagreement between the value of the angular size of the sound horizon, θ, inferred from temperature and polarization data, as well as an overall worse global fit to the different spectra.

TABLE II. Mean values and 68% CL errors on the most relevant cosmological parameters, including the growth index γ, together with the 95% CL upper limits on the total neutrino mass $\sum m_\nu$ arising from different combinations of cosmological datasets.

Parameter	Plik + DESI + PP	Plik + DESI + PP (NO)	Camspec + DESI + PP	Camspec + DESI + PP (NO)
$\Omega_b h^2$	0.02260 ± 0.00014	0.02264 ± 0.00014	0.02236 ± 0.00013	0.02240 ± 0.00013
$\Omega_c h^2$	$0.1171^{+0.0012}_{-0.00086}$	$0.1165^{+0.0010}_{-0.00079}$	$0.11740^{+0.00091}_{-0.00075}$	$0.11682^{+0.00081}_{-0.00073}$
$100\theta_{MC}$	1.04123 ± 0.00029	1.04129 ± 0.00029	1.04101 ± 0.00024	1.04106 ± 0.00023
τ	$0.0500^{+0.0085}_{-0.0074}$	$0.0502^{+0.0084}_{-0.0074}$	$0.0490^{+0.0086}_{-0.0074}$	$0.0494^{+0.0085}_{-0.0074}$
$\ln(10^{10}A_s)$	$3.027^{+0.018}_{-0.016}$	$3.026^{+0.018}_{-0.016}$	$3.024^{+0.018}_{-0.016}$	$3.023^{+0.018}_{-0.016}$
n_s	0.9726 ± 0.0038	0.9739 ± 0.0037	0.9696 ± 0.0037	0.9711 ± 0.0036
γ	0.707 ± 0.075	0.742 ± 0.069	0.660 ± 0.063	0.696 ± 0.060
$\sum m_\nu$ [eV]	< 0.188	< 0.208	< 0.134	< 0.164
Ω_m	0.2993 ± 0.0040	0.3000 ± 0.0040	0.3004 ± 0.0039	0.3016 ± 0.0038
H_0 [km/s/Mpc]	68.52 ± 0.35	68.42 ± 0.34	68.36 ± 0.32	68.21 ± 0.31
S_8	$0.791^{+0.021}_{-0.014}$	$0.780^{+0.017}_{-0.013}$	$0.798^{+0.016}_{-0.012}$	$0.787^{+0.014}_{-0.011}$

consideration, making the analysis unnecessarily cumbersome and less easy to interpret. For this reason, we restrict our analysis to Pantheon+, which is typically regarded as the more conservative catalogue, yielding constraints more consistent with Planck ΛCDM results. In contrast, DESy5 tends to favor deviations, especially in dynamical dark energy models. However, the nature of this shift remains debated. For instance, Ref. [97] links the tension with Planck ΛCDM cosmology to a ∼0.04 mag calibration offset in low-redshift DESy5 SNIa. In response to these findings, the DES Collaboration, in Ref. [197], argued that such an offset arises from improved modeling of intrinsic scatter and host galaxy properties, as well as differences in the selection functions used across different samples. While we do not take a stance on this issue, these considerations motivate our use of Pantheon+, as it offers a conservative, well-tested compilation, limits residual systematics, and avoids unnecessary complexity. Last but not least, Pantheon + yields the tightest neutrino mass constraints across both ΛCDM and dynamical dark energy scenarios (see, e.g., Ref. [47] or Table 8 of Ref. [3]).[9]

IV. RESULTS

We present our main findings in Table II, which compares the results obtained by simultaneously varying the neutrino mass and the growth index γ using different CMB likelihoods in combination with DESI BAO and Pantheon + SNIa measurements. For reference, results obtained by varying each of these parameters individually while keeping the other fixed are reported in Table III, and discussed in the Appendix. As already noted in the previous section, we consider two distinct prior choices for $\sum m_\nu$, as listed in Table I. Specifically, the label "NO" refers to the case where we impose the lower bound on $\sum m_\nu$ from particle physics experiments, i.e., enforcing a prior $\sum m_\nu > 0.06$ eV, consistent with current neutrino oscillation measurements [2].

First and foremost, we confirm that the constraints on the neutrino mass are significantly relaxed compared to the minimal ΛCDM + $\sum m_\nu$ case with the growth index fixed to $\gamma = 0.55$. When both $\sum m_\nu$ and γ are allowed to vary simultaneously, the most constraining bound, $\sum m_\nu < 0.134$ eV at 95% CL, is obtained using the Camspec likelihood in combination with DESI and PP data. This limit remains substantially larger—by more than a factor of 2—than the corresponding bound obtained for the same dataset combination when fixing $\gamma = 0.55$, which yields $\sum m_\nu < 0.0643$ eV at 95% CL, remarkably close to the lower bound expected from terrestrial measurements.

Secondly, we confirm a non-negligible dependence on the specific CMB likelihood adopted in the analysis. As shown in Table II, when varying both parameters, the bound on the neutrino mass changes from the aforementioned $\sum m_\nu < 0.134$ eV to $\sum m_\nu < 0.188$ eV upon replacing the Planck-PR4 Camspec and lensing likelihoods with the older Plik PR3 counterparts, further relaxing the upper limit on the total neutrino mass.

Either way, however, the limits on $\sum m_\nu$ remain largely consistent with the lower bounds from oscillation experiments, both within the NO and the IO, thereby alleviating the emerging tension observed in ΛCDM. Therefore, we can relatively safely apply the NO prior in the analysis and enforce $\sum m_\nu > 0.06$ eV. Doing so, the neutrino mass bound from Camspec + DESI + PP becomes further relaxed to $\sum m_\nu < 0.164$ eV, implying a shift of about 0.03 eV towards larger mass values. Similarly, when enforcing the NO prior, the bound obtained from Plik + DESI + PP becomes $\sum m_\nu < 0.208$ eV, corresponding to a shift of approximately 0.02 eV. For both cases, the size and magnitude of this shift can be seen in Fig. 3, which shows the 2D 68% and 95% probability contours in the (γ, $\sum m_\nu$) plane. Specifically, in the left panel, the solid green contours correspond to the results obtained from

[9]For example, combining CMB and DESI with Pantheon + gives $\sum m_\nu < 0.117$ eV in the dynamical dark energy model, while DESy5 leads to $\sum m_\nu < 0.129$ eV [47].

TABLE III. Mean values and 68% CL errors on the most relevant cosmological parameters, including the growth index γ, together with the 95% CL upper limits on the total neutrino mass $\sum m_\nu$ arising from different combinations of cosmological datasets.

Parameter	$\Lambda\mathrm{CDM}+\sum m_\nu$		$\Lambda\mathrm{CDM}+\gamma$	
	Plik + DESI + PP	Camspec + DESI + PP	Plik + DESI + PP	Camspec + DESI + PP
$\Omega_b h^2$	0.02250 ± 0.00013	0.02229 ± 0.00012	0.02258 ± 0.00013	0.02237 ± 0.00012
$\Omega_c h^2$	0.11824 ± 0.00067	0.11815 ± 0.00064	0.11734 ± 0.00066	0.11733 ± 0.00064
$100\theta_{MC}$	1.04116 ± 0.00028	1.04096 ± 0.00023	1.04121 ± 0.00028	1.04101 ± 0.00023
τ	$0.0580^{+0.0066}_{-0.0075}$	0.0561 ± 0.0069	$0.0498^{+0.0085}_{-0.0075}$	$0.0488^{+0.0085}_{-0.0073}$
$\log(10^{10}A_s)$	3.048 ± 0.014	3.042 ± 0.014	$3.028^{+0.018}_{-0.016}$	$3.024^{+0.018}_{-0.015}$
n_s	0.9694 ± 0.0033	0.9676 ± 0.0034	0.9719 ± 0.0033	0.9698 ± 0.0035
$\sum m_\nu$ [eV]	< 0.0710	< 0.0643	0.06	0.06
γ	0.55	0.55	0.692 ± 0.056	0.666 ± 0.052
Ω_m	0.3009 ± 0.0037	0.3018 ± 0.0036	0.2990 ± 0.0038	0.3006 ± 0.0037
H_0 [Km/s/Mpc]	68.47 ± 0.30	68.28 ± 0.29	68.57 ± 0.30	68.34 ± 0.29
S_8	0.8167 ± 0.0090	0.8157 ± 0.0082	0.796 ± 0.010	0.796 ± 0.010

Plik + DESI + PP, while the empty dashed gray contours illustrate how these results shift when a NO prior is imposed. Similarly, the solid red contours in the right panel show the constraints from Camspec + DESI + PP, and the gray contours indicate how they change when enforcing $\sum m_\nu > 0.06$ eV. Clearly, the impact of the prior is more pronounced in the Camspec-based results.

Most importantly, as clearly seen from the two-dimensional allowed regions in Fig. 3, there is a strong positive correlation between γ and $\sum m_\nu$: larger values of the total neutrino mass imply a suppression of the growth of structure in the Universe, which can be compensated by a higher growth index. Therefore, when it comes to the growth index γ, several interesting observations are in order. Firstly, using the Camspec likelihood in combination with DESI and SNIa observations (without assuming a NO prior on the neutrino mass), we obtain $\gamma = 0.660 \pm 0.063$ at 68% CL, indicating a $\sim 1.8\sigma$ shift from the standard growth rate model. This shift increases to $\sim 2.1\sigma$ when replacing Camspec with Plik, which yields $\gamma = 0.707 \pm 0.075$ at 68% CL. Due to the strong positive correlation between γ and $\sum m_\nu$, this tendency towards a larger

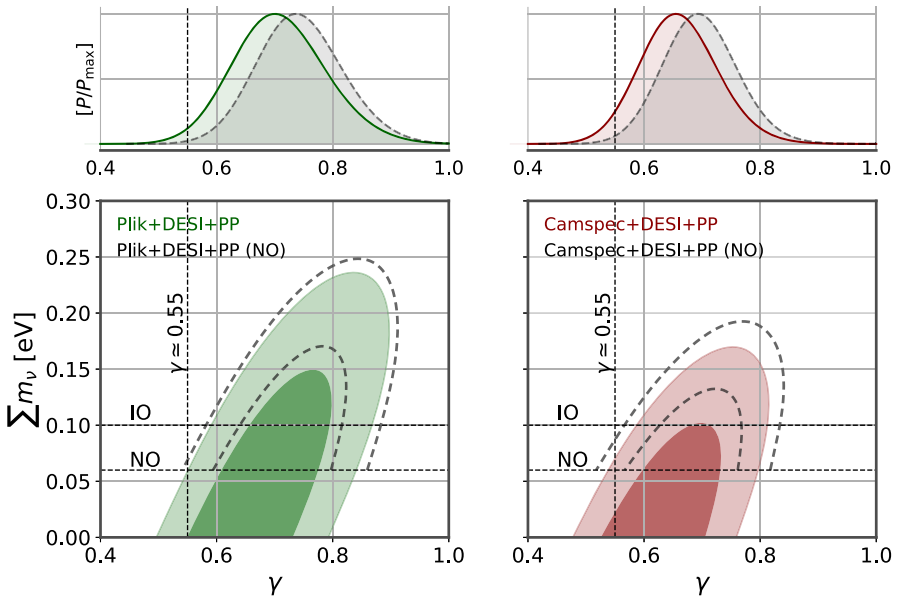

FIG. 3. One-dimensional marginalized posterior distributions and two-dimensional 68% and 95% CL contours in the $(\gamma, \sum m_\nu)$ plane for different Planck CMB likelihoods combined with DESI and PP data. The horizontal black dashed line labeled "NO" marks the lower bound on the total neutrino mass set by oscillation experiments ($\sum m_\nu > 0.06$ eV). Values below this line are therefore in tension with oscillation data. Instead, the horizontal black dashed line labeled "IO" indicates the lowest value of the total neutrino mass compatible with the inverted ordering ($\sum m_\nu > 0.1$ eV). If the total neutrino mass lies between the NO and IO lines, only the normal ordering is allowed, whereas for values above the IO line both orderings remain viable. The vertical black dashed line corresponds to the standard prediction for the growth index ($\gamma \simeq 0.55$).

growth index becomes significantly more pronounced when enforcing a NO prior on $\sum m_\nu$. For Camspec + DESI + PP we obtain $\gamma = 0.696 \pm 0.060$, while for Plik + DESI + PP, we get $\gamma = 0.742 \pm 0.069$—i.e., $\sim 2.4\sigma$ and $\sim 2.8\sigma$ away from the expected value of $\gamma = 0.55$, respectively. This further shift towards larger values of γ induced by the NO prior can be clearly seen in the 1D posterior distributions shown in the top histograms of Fig. 3. In both the left and right panels, the dashed gray curves (corresponding to the analysis with the NO prior) are visibly shifted towards higher values of γ compared to the distributions obtained when this prior is not applied.

The situation becomes even more intriguing when examining the 2D contours in Fig. 3 for the different cases. As already noted, allowing for a nonstandard growth of structure can reconcile the current tension in the neutrino sector: even in the most constraining scenario, the cosmological bounds on neutrino masses remain fully compatible with laboratory results, showing no conflict between cosmological and terrestrial constraints. However, this agreement comes at the cost of departing from the standard structure growth predicted in ΛCDM. As illustrated in the figure, the point defined by the intersection of $\gamma = 0.55$ (i.e., the baseline prediction for the growth index) and $\sum m_\nu = 0.06$ eV (i.e., the minimal mass allowed by oscillation experiments) lies literally at the boundary of the 95% confidence region for Plik + DESI + PP (i.e., the combination allowing the most freedom in the neutrino mass), and very close to the boundary for Camspec + DESI + PP. This means that any neutrino mass value larger than this lower limit would necessarily require a larger γ, thus moving away from ΛCDM predictions for structure formation. Conversely, if we wish to remain consistent with $\gamma = 0.55$ (i.e., following the vertical black dashed line in the figure), the only viable region lies below $\sum m_\nu = 0.06$ eV, thereby reintroducing the tension with oscillation experiments. Similarly, as far as the mass ordering is concerned, while the 95% CL upper bounds on $\sum m_\nu$ remain consistent with both NO and IO, crossing the lower limit set by oscillation experiments within the IO necessarily implies a departure from standard structure formation growth within this framework. Indeed, it is crucial to note that the point defined by $\gamma = 0.55$ and $\sum m_\nu = 0.1$ eV (i.e., the minimal mass allowed within the IO) always lies well outside the 95% probability contours and consistency with the IO (i.e., restricting attention to the region of the plane above the corresponding horizontal line in Fig. 3) necessarily implies values of γ significantly larger than those predicted by ΛCDM.

We now turn to a broader exploration of the implications of allowing departures from the standard structure growth history, focusing on additional parameters of interest for other outstanding cosmological tensions. We begin with the $S_8 \equiv \sigma_8(\Omega_m/0.3)^{0.5}$ parameter that quantifies the amplitude of matter fluctuations on intermediate scales and which has played a central role in the longstanding discussions surrounding potential discrepancies between CMB-derived results and weak lensing survey estimates [198–217]. As shown in Fig. 4, we observe a strong anticorrelation between γ and S_8. Larger values of the growth index tend to favour both larger values of the total neutrino mass (see Fig. 3) and smaller values of S_8. Quantitatively, for Plik + DESI + PP, we find $S_8 = 0.791^{+0.021}_{-0.014}$, which reduces to $S_8 = 0.780^{+0.017}_{-0.013}$ when assuming a NO prior. Similarly, for the Camspec likelihood, we obtain $S_8 = 0.798^{+0.016}_{-0.012}$ without prior assumptions, shifting to $S_8 = 0.787^{+0.014}_{-0.011}$ under the NO prior. In both cases, as seen in Fig. 4, the NO prior leads to a noticeable drift of the posteriors toward lower S_8 values and away from the canonical GR limit $\gamma = 0.55$, echoing the behaviour already discussed in previous sections. This interplay between γ, $\sum m_\nu$, and S_8 can be particularly relevant in light of ongoing discussions about the persistence of the weak lensing discrepancy, generalizing the discussion presented in Refs. [160,161] to massive neutrino cosmologies. Despite recent claims suggesting this tension may have been alleviated or even resolved [217,218], our results indicate that the inclusion of a flexible growth history introduces parameter shifts in a direction potentially capable of reconciling lensing data with CMB-derived inferences, should the discrepancy persist. If we aim to be more quantitative in assessing the extent to which varying γ alleviates the S_8 tension, we should first note that weak-lensing surveys report somewhat different determinations of S_8. To mention a few concrete examples, KiDS-1000 in combination with 2dFLenS and BOSS yields $S_8 = 0.766^{+0.020}_{-0.014}$ [209], the DES-Y3 3×2pt analysis gives $S_8 = 0.776 \pm 0.017$ [216], while the more recent KiDS-Legacy release finds $S_8 = 0.815^{+0.016}_{-0.021}$ [217], which, as mentioned above, shows no discrepancy with the ΛCDM Planck-only based inferences of $S_8 = 0.834 \pm 0.016$ [21].[10] A direct quantification of the tension is therefore nontrivial, not only because of these differing estimates but also because S_8 is itself a model-dependent parameter. As such, a fully consistent comparison would require reanalyzing the weak-lensing data within the same theoretical framework adopted here, which lies well beyond the scope of this manuscript. Nevertheless, even accounting for these caveats, one can clearly see that the results presented in the Appendix, Table III, obtained for fixed $\gamma = 0.55$, yield values scattered around $S_8 \simeq 0.816$ that, considering the uncertainties, remain in a ~ 2.1–2.3σ tension with KiDS − 1000 + 2dFLenS + BOSS and DES-Y3, while being in good agreement with KiDS-Legacy. By contrast, when allowing the growth index γ to vary freely, the inferred values shift to $S_8 \simeq 0.79$–0.80, consistently lying within $\lesssim 1\sigma$ of all weak-lensing determinations. This

[10]For a more comprehensive review of S_8 measurements from different weak-lensing surveys, see Ref. [113].

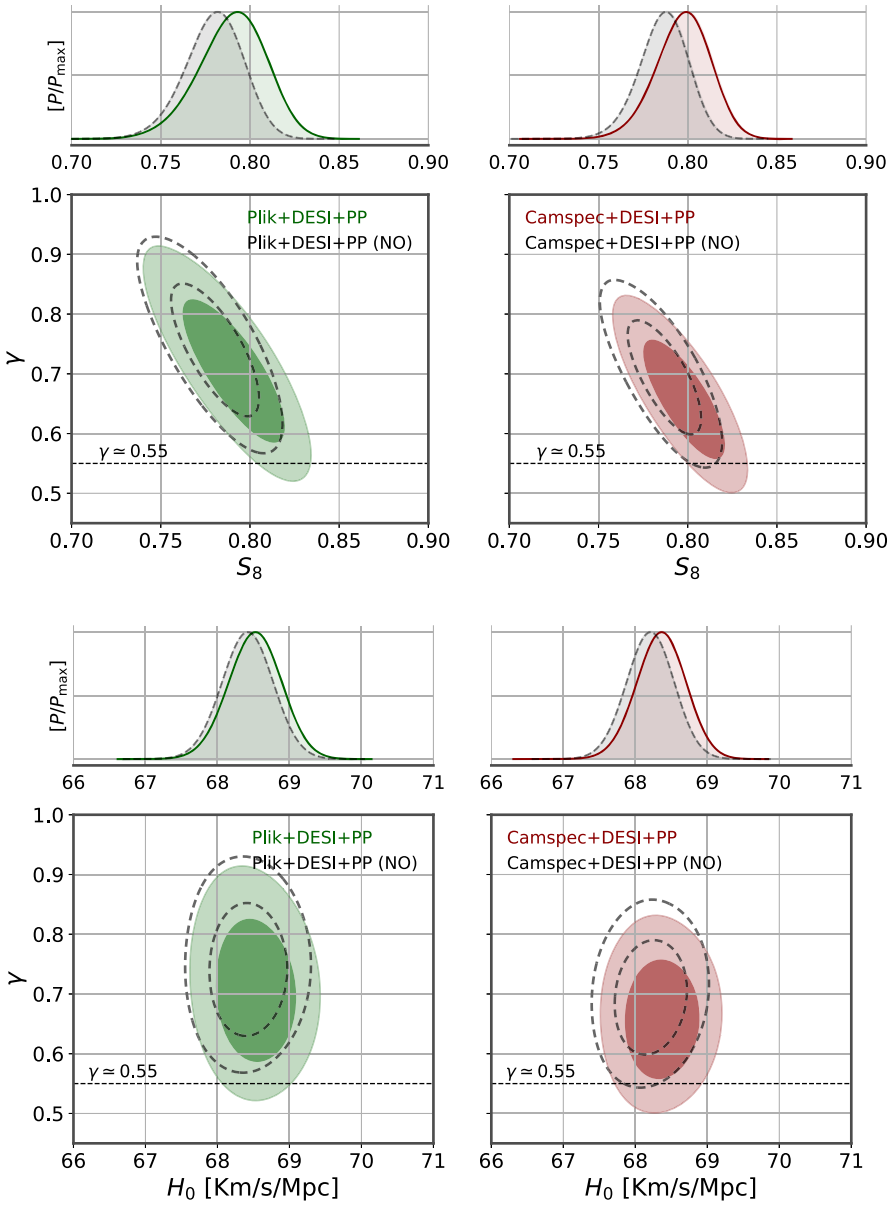

FIG. 4. One-dimensional marginalized posterior distributions and two-dimensional 68% and 95% CL probability contours for γ and S_8 (top panels) and γ and H_0 (bottom panels) for the different Planck CMB likelihoods combined with DESI and PP. The horizontal black dashed line corresponds to the standard prediction for the growth index, $\gamma \simeq 0.55$.

heuristic argument shows that a flexible growth history can naturally drive the inferred clustering amplitude toward substantially improved consistency with lensing observations. More broadly, this drift underscores the relevance of neutrino physics assumptions in any interpretation of the weak lensing tension, and the model dependence of derived parameters such as S_8. Taken together, these findings suggest that S_8 remains sensitive to beyond-ΛCDM physics, particularly when degrees of freedom such as modified growth or noncanonical neutrino properties are considered.

In contrast to the behaviour observed for S_8, we do not find any significant correlation between γ and H_0 in our analysis. The values we obtain remain remarkably stable across datasets and assumptions. For Plik + DESI + PP, we find $H_0 = 68.52 \pm 0.35$ Km/s/Mpc, shifting only slightly to $H_0 = 68.42 \pm 0.34$ Km/s/Mpc when a NO prior is imposed. Similarly, for Camspec + DESI + PP, we obtain $H_0 = 68.36 \pm 0.32$ Km/s/Mpc (without prior assumptions), decreasing mildly to $H_0 = 68.21 \pm 0.31$ Km/s/Mpc under the NO prior. These minor shifts can be traced back to the known negative correlation between H_0 and $\sum m_\nu$, and are not driven by the growth index itself. As such, while an alternative structure growth model with a free γ can relax the neutrino mass bounds and might remain of interest in relation to the weak lensing discrepancy (should this issue persist rather than fade

definitively), it does not provide a mechanism for addressing the Hubble tension. The path toward a coherent explanation capable of simultaneously accounting for all current anomalies remains, at present, largely unfulfilled.

Last but not least, it is important to consider the matter density parameter $\Omega_{\rm m}$, as it plays a key role in the interpretation of our results and lies at the heart of the broader discussion on the neutrino mass tension. As seen by comparing the values given in Table II (as well as in Table III in the Appendix) across all the parameter spaces explored and for all combinations of datasets, we find values of $\Omega_{\rm m}$ that are consistent within one standard deviation. Specifically, when varying only the total neutrino mass, we find $\Omega_{\rm m} = 0.3009 \pm 0.0037$ for Plik + DESI + PP and $\Omega_{\rm m} = 0.3018 \pm 0.0036$ for Camspec + DESI + PP. When varying only the growth index γ, these values remain essentially unchanged: $\Omega_{\rm m} = 0.2990 \pm 0.0038$ (Plik + DESI + PP) and $\Omega_{\rm m} = 0.3006 \pm 0.0037$ (Camspec + DESI + PP).[11] Finally, when both γ and $\sum m_\nu$ are varied simultaneously, we obtain consistent values such as $\Omega_{\rm m} = 0.2993 \pm 0.0040$ (Plik + DESI + PP) and $\Omega_{\rm m} = 0.3004 \pm 0.0039$ (Camspec + DESI + PP). Under the NO prior, these latter two values shift only mildly to $\Omega_{\rm m} = 0.3000 \pm 0.0040$ and $\Omega_{\rm m} = 0.3016 \pm 0.0038$, respectively. These results illustrate a crucial point: fixing or varying γ alongside the total neutrino mass does not significantly alter the inferred value of $\Omega_{\rm m}$. However, this consistency hides an important distinction. Fixing $\gamma = 0.55$ leads to neutrino mass bounds that are very close to lower limits from particle physics experiments, to the extent of raising a very concerning tension. Conversely, allowing γ to vary relaxes this problem *without* changing the value of $\Omega_{\rm m}$. This finding directly challenges the often-stated claim that the neutrino mass tension originates from constraints on $\Omega_{\rm m}$ inferred from different probes under the assumption of a ΛCDM background. We show that this is true if one also assumes a standard ΛCDM structure formation history. Once this assumption is relaxed, the tension in $\sum m_\nu$ can be alleviated without altering the background evolution. More broadly, our results demonstrate that it is possible to relax constraints on the total neutrino mass by modifying the structure growth history, without changing the inferred values of parameters describing the background dynamics and without invoking additional degrees of freedom at the background level, such as scenarios involving dynamical dark energy. This offers a complementary path to addressing the neutrino mass problem, shifting the attention to the important imprints of neutrinos on perturbation-level observables rather than on the background expansion itself. Exploring this interplay between perturbation-level and background-level modifications is crucial, as changes to the expansion history that help relax neutrino mass bounds often come at the cost of lowering H_0 further, thereby exacerbating the Hubble tension. If the goal is to retain enough freedom to simultaneously address multiple anomalies within a coherent framework, it becomes essential to introduce the necessary degrees of freedom and explore both aspects. In this sense, alternative structure formation histories may offer a viable and physically well-motivated possibility.

[11]We note that the tendency toward larger values of the growth index γ is also present when fixing the total neutrino mass in the cosmological model, and that it persists regardless of the CMB likelihood employed; see the discussion in the Appendix.

V. SUMMARY

Assuming the minimal ΛCDM framework with three degenerate massive neutrinos, the DESI Collaboration recently reported an upper bound of $\sum m_\nu \lesssim 0.064$ eV at 95% CL when combining DESI-2025 BAO data with Planck-PR4 CMB observations. This bound is uncomfortably close to the lower limit set by oscillation experiments in the case of normal ordering and firmly excludes the inverted ordering, thus raising serious concerns. In particular, it has been argued that these tight limits mainly stem from a mild but persistent mismatch in the preferred matter density: BAO measurements from DESI favor lower values of $\Omega_{\rm m}$ than those inferred from the CMB, resulting in an indirect pressure toward smaller values of $\sum m_\nu$.

An appealing way to alleviate this issue is to consider extensions beyond the standard cosmological framework. Models featuring dynamical dark energy, which modify the late-time expansion history of the Universe, can significantly relax the neutrino mass bounds and reduce the tension. Therefore, the mainstream (but far from universally accepted) interpretation is that the unnaturally low bounds on $\sum m_\nu$ may themselves point to the failure of ΛCDM to accurately describe the expansion history at late times. However, matter density and massive neutrinos do not only affect the background evolution, but also play crucial roles in the growth of cosmic structure: matter density drives the gravitational clustering of overdensities, while massive neutrinos suppress the formation of structure at small scales due to their large thermal velocities. Therefore, new physics affecting the dynamics of primordial perturbations and structure formation can offer a complementary possibility to alleviate the neutrino mass tension.

In this paper, we explore this possibility by considering a flexible, phenomenological approach to structure growth by allowing the growth rate $f(a)$ to depart from its ΛCDM prediction. Specifically, we parametrize it using the growth index γ through $f(a) \simeq \Omega_{\rm m}(a)^\gamma$ and treat γ as a free parameter. A larger value of γ suppresses the growth rate, implying a larger growth function in the past and modifying the way matter perturbations cluster in the (early) Universe. This, in turn, affects both the high-multipole CMB lensing signal and the shape of the matter power spectrum. Such effects can be compensated by a larger neutrino mass. In this regard, it is important to emphasize the role of CMB lensing in driving the neutrino mass bounds, particularly when the growth index is fixed to its standard value. The lensing potential encodes the integrated matter distribution

along the line of sight and is especially sensitive to the amplitude of clustering on intermediate and small scales. Since massive neutrinos suppress structure growth, their effect is clearly imprinted in the lensing signal at high multipoles. In the standard scenario with $\gamma = 0.55$, any deviation from the measured lensing power is necessarily attributed to a lower neutrino mass, thereby tightening the constraint on $\sum m_\nu$. However, when γ is allowed to vary, structure suppression can be partially absorbed by a larger growth index, weakening the need for extremely small neutrino masses. This illustrates how perturbation-level flexibility, especially in structure growth, can mitigate tensions that appear under stricter assumptions.

Our main results can be summarized as follows:

(i) By jointly varying $\sum m_\nu$ and the growth index γ, we find that the cosmological bounds on the total neutrino mass are substantially relaxed compared to the standard case. Across all combinations of Planck-CMB, DESI-BAO, and Pantheon + SNIa data, we find that allowing γ to vary broadens the allowed range for $\sum m_\nu$ from ∼0.06–0.07 eV (assuming $\gamma = 0.55$) up to ∼0.13–0.2 eV. These values are consistent with terrestrial constraints and demonstrate that new physics at the perturbation level offers a viable, complementary solution to the neutrino mass tension.

(ii) This agreement, however, comes at the cost of deviating from the standard structure growth predictions of ΛCDM. As shown in Fig. 3, the point defined by $\gamma = 0.55$ (i.e., the baseline value of γ) and $\sum m_\nu = 0.06$ eV (i.e., the lowest total neutrino mass allowed by particle physics experiments) lies on the boundary of the 95% confidence region. This means that any neutrino mass value larger than this lower limit would necessarily require a larger γ, thus moving away from ΛCDM predictions for structure formation. Conversely, if we wish to remain consistent with $\gamma = 0.55$, the only viable region lies below $\sum m_\nu = 0.06$ eV, reintroducing the tension with oscillation experiments.

(iii) Regarding the neutrino mass ordering, we find that the inverted ordering remains allowed within modified structure growth models. However, accommodating mass values consistent with the inverted ordering requires values of γ significantly larger than the ΛCDM prediction.

(iv) Overall, we observe a consistent trend favouring larger-than-standard values of γ. This preference persists whether one varies only γ or both γ and $\sum m_\nu$ simultaneously. In the latter case, the preference reaches 1.8σ for Plik + DESI + PP and 2σ for Camspec + DESI + PP. Imposing a prior consistent with normal ordering ($\sum m_\nu > 0.06$ eV) strengthens the preference further, up to 2.4σ and 2.8σ, respectively.

(v) Importantly, we find that allowing γ to vary relaxes the neutrino mass bounds without altering the inferred value of Ω_m. This is clearly seen by comparing the values reported in Tables II and III. While previous studies attributed the tight neutrino mass bounds to the ability of ΛCDM to accurately describe the late-time background dynamics, we show that this interpretation only holds under the assumption of standard ΛCDM structure growth. Once this assumption is relaxed, the tension can be alleviated without modifying the ΛCDM background evolution.

(vi) Last but not least, Fig. 4 reveals a strong anticorrelation between γ and S_8: larger growth indices lead to both larger allowed neutrino masses and smaller values of S_8. This interplay may be relevant for the ongoing debate about the weak lensing anomaly. While some recent analyses suggest that the S_8 tension may be subsiding, our results indicate that a flexible growth history can still shift parameters in a direction that could better reconcile lensing and CMB data, if the tension persists. On the other hand, we find no significant correlation between γ and H_0, implying that growth index freedom does not offer a mechanism for addressing the Hubble tension.

All in all, in the absence of a definitive cosmological detection of neutrino mass, our analysis provides a novel and complementary angle on the tension between cosmology and particle physics. It highlights the critical role of perturbations in constraining new physics and underscores the importance of testing both the background and structure formation histories when interpreting cosmological data. As future observations improve and our modeling of structure formation becomes more refined, noncanonical scenarios (e.g., modified theories of gravity or a nonminimal dark sector) may well emerge as essential components of a more complete cosmological paradigm that accurately accounts for massive neutrinos.

ACKNOWLEDGMENTS

W. G. is supported by the Lancaster Sheffield Consortium for Fundamental Physics under STFC Grant No. ST/X000621/1. O. M. acknowledges the financial support from the MCIU with funding from the European Union NextGenerationEU (PRTR-C17.I01) and Generalitat Valenciana (ASFAE/2022/020). E. D. V. is supported by a Royal Society Dorothy Hodgkin Research Fellowship. This work has been supported also by the Spanish MCIN/AEI/10.13039/501100011033 Grants No. PID2020–113644 GB-I00, No. ID2023-148162NB-C21, and No. PID2023-148162NB-C22, and by the European ITN Project HIDDeN (H2020-MSCA-ITN-2019/860881-HIDDeN) and SE Project ASYMMETRY (HORIZON-MSCA-2021-SE-01/101086085-ASYMMETRY) and well as by the Generalitat Valenciana Grants No. PROMETEO/

2019/083, No. PROMETEO/2021/083, and No. CIPROM/2022/69. O. M. acknowledges the financial support from the MCIU with funding from the European Union NextGenerationEU (PRTR-C17.I01) and Generalitat Valenciana (ASFAE/2022/020) We acknowledge the IT Services at The University of Sheffield for the provision of services for High Performance Computing. This article is based upon work from the COST Action CA21136—"Addressing observational tensions in cosmology with systematics and fundamental physics (CosmoVerse)", supported by COST—"European Cooperation in Science and Technology."

DATA AVAILABILITY

The data that support the findings of this article are openly available [47].

APPENDIX: FULL ANALYSIS RESULTS

In this appendix, we briefly illustrate the cosmological constraints on the growth index γ and on the total neutrino mass $\sum m_\nu$ for cosmological scenarios in which only one between $\sum m_\nu$ and γ is allowed to vary freely while the other is kept fixed in the model.

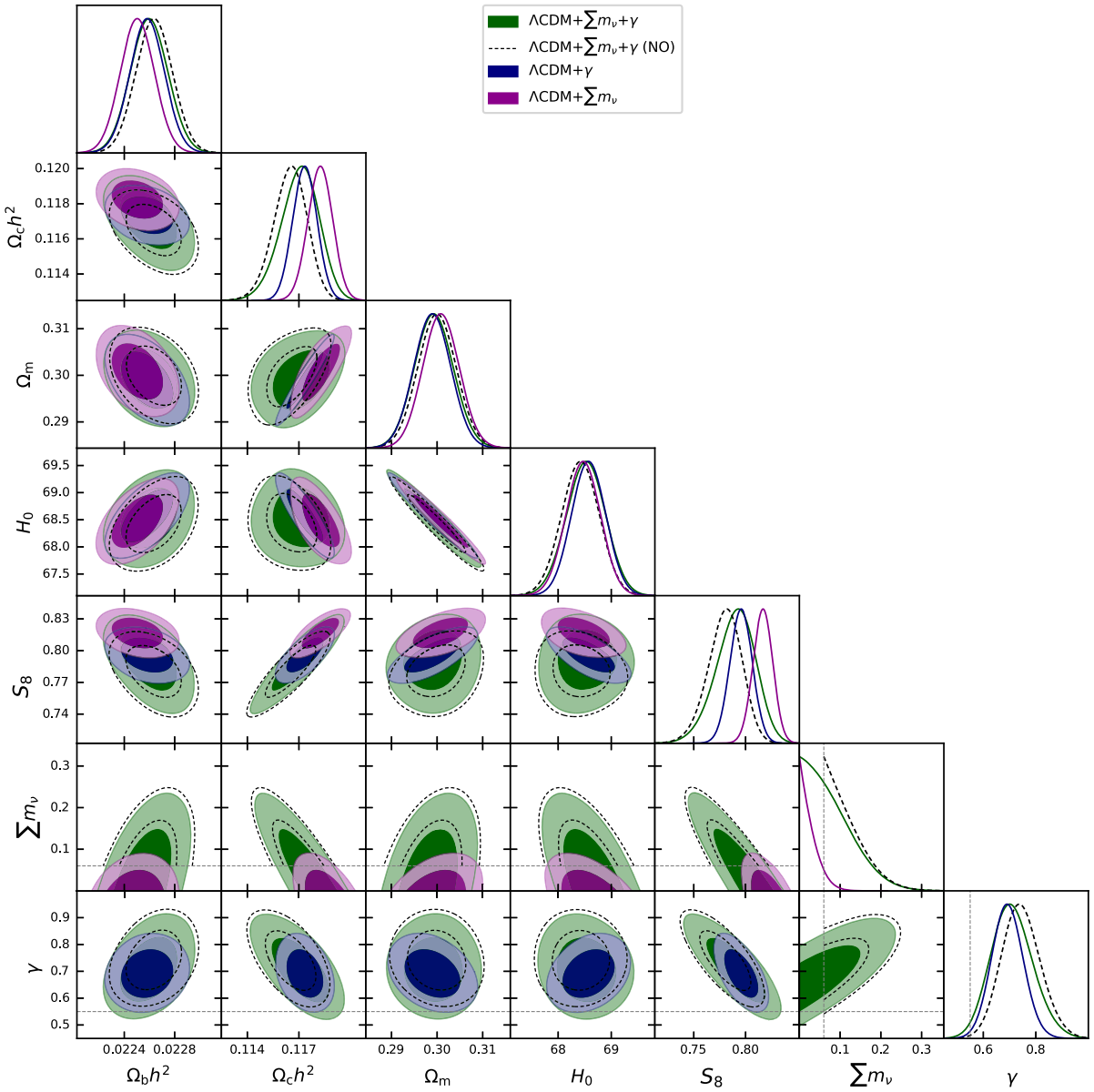

FIG. 5. One-dimensional marginalized posterior distributions and two-dimensional 68% and 95% CL contours for several cosmological parameters of interest, obtained from the analysis of Plik + DESI + PP under the different cosmological models and prior choices indicated in the figure legend. The dashed gray lines denote the lower bound on the total neutrino mass from oscillation experiments ($\sum m_\nu \simeq 0.06$ eV) and the standard ΛCDM prediction for the growth index ($\gamma = 0.55$).

We show in Table III, the main results obtained in this scenario, while Figs. 5 and 6 display the one-dimensional distribution functions and the two-dimensional probability contours obtained for the different models (including the case where both γ and $\sum m_\nu$ are varied simultaneously), for Plik + DESI + PP and Camspec + DESI + PP, respectively.

Focusing on the neutrino mass constraints within a Universe with a standard growth index $\gamma = 0.55$, we find extremely tight bounds on $\sum m_\nu$ for both the Camspec and Plik CMB likelihoods. These 95% CL upper limits are $\sum m_\nu < 0.0643$ eV for Camspec + DESI + PP, and slightly relaxed to $\sum m_\nu < 0.0710$ eV for Plik + DESI + PP. In either case, the limits are close to the minimum bound expected from neutrino oscillation experiments, $\sum m_\nu > 0.06$ eV, hinting at a mild tension.

In the complementary case where the total neutrino mass is fixed to $\sum m_\nu = 0.06$ eV and the growth index is allowed to vary, the tendency toward larger values of γ is confirmed. Indeed, we find $\gamma = 0.692 \pm 0.056$ for Plik + DESI + PP and $\gamma = 0.666 \pm 0.052$ for Camspec + DESI + PP, deviating from the expected value by $\sim 2.5\sigma$ and $\sim 2.2\sigma$, respectively.

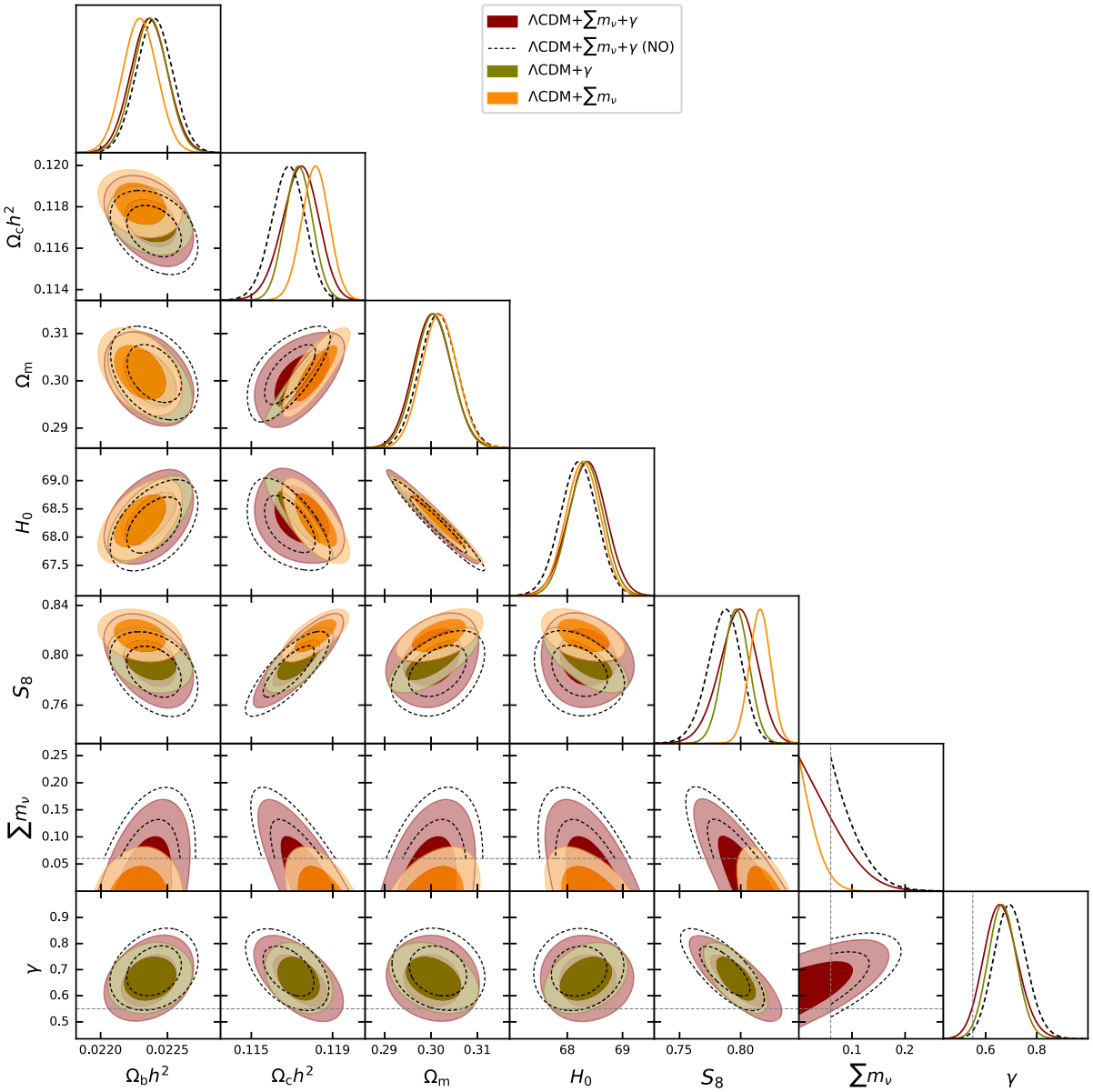

FIG. 6. One-dimensional marginalized posterior distributions and two-dimensional 68% and 95% CL contours for several cosmological parameters of interest, obtained from the analysis of Camspec + DESI + PP under the different cosmological models and prior choices indicated in the figure legend. The dashed gray lines denote the lower bound on the total neutrino mass from oscillation experiments ($\sum m_\nu \simeq 0.06$ eV) and the standard ΛCDM prediction for the growth index ($\gamma = 0.55$).

As for the correlations between γ and the remaining cosmological parameters, they behave as expected: as seen both in Fig. 5 and Fig. 6 γ is negatively correlated with $\Omega_c h^2$, due to the growth rate being parametrized as $\Omega_m(a)^\gamma$.

[1] P. F. de Salas, D. V. Forero, S. Gariazzo, P. Martínez-Miravé, O. Mena, C. A. Ternes, M. Tórtola, and J. W. F. Valle, J. High Energy Phys. 02 (2021) 071.
[2] I. Esteban, M. C. Gonzalez-Garcia, M. Maltoni, I. Martinez-Soler, J. P. Pinheiro, and T. Schwetz, J. High Energy Phys. 12 (2024) 216.
[3] F. Capozzi, W. Giarè, E. Lisi, A. Marrone, A. Melchiorri, and A. Palazzo, Phys. Rev. D **111**, 093006 (2025).
[4] S. Weinberg, Phys. Rev. Lett. **43**, 1566 (1979).
[5] P. Minkowski, Phys. Lett. **67B**, 421 (1977).
[6] R. N. Mohapatra and G. Senjanovic, Phys. Rev. Lett. **44**, 912 (1980).
[7] M. Gell-Mann, P. Ramond, and R. Slansky, Conf. Proc. C **790927**, 315 (1979).
[8] S. F. King, arXiv:2502.07877.
[9] F. F. Deppisch, M. Hirsch, and H. Pas, J. Phys. G **39**, 124007 (2012).
[10] S. Dell'Oro, S. Marcocci, M. Viel, and F. Vissani, Adv. High Energy Phys. **2016**, 2162659 (2016).
[11] K. Abe *et al.* (T2K Collaboration), Eur. Phys. J. C **83**, 782 (2023).
[12] M. A. Acero *et al.* (NOvA Collaboration), Phys. Rev. D **106**, 032004 (2022).
[13] F. An *et al.* (JUNO Collaboration), J. Phys. G **43**, 030401 (2016).
[14] K. Abe *et al.* (Hyper-Kamiokande Collaboration), arXiv:1805.04163.
[15] B. Abi *et al.* (DUNE Collaboration), arXiv:2002.03005.
[16] S. Gariazzo, M. Archidiacono, P. F. de Salas, O. Mena, C. A. Ternes, and M. Tórtola, J. Cosmol. Astropart. Phys. 03 (2018) 011.
[17] M. Aker *et al.* (KATRIN Collaboration), Science **388**, adq9592 (2025).
[18] W. Elbers *et al.* (DESI Collaboration), Phys. Rev. D **112**, 083513 (2025).
[19] D. Wang, O. Mena, E. Di Valentino, and S. Gariazzo, Phys. Rev. D **110**, 103536 (2024).
[20] J.-Q. Jiang, W. Giarè, S. Gariazzo, M. G. Dainotti, E. Di Valentino, O. Mena, D. Pedrotti, S. S. da Costa, and S. Vagnozzi, J. Cosmol. Astropart. Phys. 01 (2025) 153.
[21] N. Aghanim *et al.* (Planck Collaboration), Astron. Astrophys. **641**, A6 (2020); **652**, C4(E) (2021).
[22] N. Palanque-Delabrouille, C. Yèche, N. Schöneberg, J. Lesgourgues, M. Walther, S. Chabanier, and E. Armengaud, J. Cosmol. Astropart. Phys. 04 (2020) 038.
[23] E. Di Valentino, S. Gariazzo, and O. Mena, Phys. Rev. D **104**, 083504 (2021).
[24] S. Brieden, H. Gil-Marín, and L. Verde, J. Cosmol. Astropart. Phys. 08 (2022) 024.
[25] M. Loverde and Z. J. Weiner, J. Cosmol. Astropart. Phys. 12 (2024) 048.
[26] N. Craig, D. Green, J. Meyers, and S. Rajendran, J. High Energy Phys. 09 (2024) 097.
[27] D. Naredo-Tuero, M. Escudero, Enrique Fernández-Martínez, X. Marcano, and V. Poulin, Phys. Rev. D **110**, 123537 (2024).
[28] D. Green and J. Meyers, Phys. Rev. D **111**, 083507 (2025).
[29] W. Elbers, C. S. Frenk, A. Jenkins, B. Li, and S. Pascoli, Phys. Rev. D **111**, 063534 (2025).
[30] E. Ó. Colgáin and M. M. Sheikh-Jabbari, arXiv:2412.12905.
[31] G. P. Lynch and L. Knox, Phys. Rev. D **112**, 083543 (2025).
[32] N. Sailer, G. S. Farren, S. Ferraro, and M. White, arXiv:2504.16932.
[33] T. Jhaveri, T. Karwal, and W. Hu, Phys. Rev. D **112**, 043541 (2025).
[34] Z. Wang, S. Lin, Z. Ding, and B. Hu, Mon. Not. R. Astron. Soc. **534**, 3869 (2024).
[35] E. Ó. Colgáin, M. G. Dainotti, S. Capozziello, S. Pourojaghi, M. M. Sheikh-Jabbari, and D. Stojkovic, J. High Energy Astrophys. **49**, 100428 (2026).
[36] D. Sapone and S. Nesseris, Phys. Rev. D **112**, 063523 (2025).
[37] E. Ó. Colgáin, S. Pourojaghi, and M. M. Sheikh-Jabbari, arXiv:2505.19029.
[38] E. Ó. Colgáin, S. Pourojaghi, M. M. Sheikh-Jabbari, and L. Yin, arXiv:2504.04417.
[39] W. Giarè, T. Mahassen, E. Di Valentino, and S. Pan, Phys. Dark Universe **48**, 101906 (2025).
[40] G. Efstathiou, arXiv:2505.02658.
[41] W. Giarè, arXiv:2409.17074.
[42] W. Giarè, E. Di Valentino, and A. Melchiorri, Phys. Rev. D **109**, 103519 (2024).
[43] S. Roy Choudhury and T. Okumura, Astrophys. J. Lett. **976**, L11 (2024).
[44] S. Gariazzo, W. Giarè, O. Mena, and E. Di Valentino, Phys. Rev. D **111**, 023540 (2025).
[45] S. Roy Choudhury, Astrophys. J. Lett. **986**, L31 (2025).
[46] A. G. Adame *et al.* (DESI Collaboration), J. Cosmol. Astropart. Phys. 02 (2025) 021.
[47] M. Abdul Karim *et al.* (DESI Collaboration), Phys. Rev. D **112**, 083515 (2025).
[48] G. Gu *et al.* (DESI Collaboration), arXiv:2504.06118.
[49] M. Cortês and A. R. Liddle, J. Cosmol. Astropart. Phys. 12 (2024) 007.
[50] D. Shlivko and P. J. Steinhardt, Phys. Lett. B **855**, 138826 (2024).
[51] O. Luongo and M. Muccino, Astron. Astrophys. **690**, A40 (2024).
[52] W. Yin, J. High Energy Phys. 05 (2024) 327.

[53] I. D. Gialamas, G. Hütsi, K. Kannike, A. Racioppi, M. Raidal, M. Vasar, and H. Veermäe, Phys. Rev. D **111**, 043540 (2025).
[54] B. R. Dinda, J. Cosmol. Astropart. Phys. 09 (2024) 062.
[55] M. Najafi, S. Pan, E. Di Valentino, and J. T. Firouzjaee, Phys. Dark Universe **45**, 101539 (2024).
[56] H. Wang and Y.-S. Piao, arXiv:2404.18579.
[57] G. Ye, M. Martinelli, B. Hu, and A. Silvestri, Phys. Rev. Lett. **134**, 181002 (2025).
[58] Y. Tada and T. Terada, Phys. Rev. D **109**, L121305 (2024).
[59] Y. Carloni, O. Luongo, and M. Muccino, Phys. Rev. D **111**, 023512 (2025).
[60] C.-G. Park, J. C. Pérez, and B. Ratra, Phys. Rev. D **110**, 123533 (2024).
[61] K. Lodha *et al.* (DESI Collaboration), Phys. Rev. D **111**, 023532 (2025).
[62] S. Bhattacharya, G. Borghetto, A. Malhotra, S. Parameswaran, G. Tasinato, and I. Zavala, J. Cosmol. Astropart. Phys. 09 (2024) 073.
[63] O. F. Ramadan, J. Sakstein, and D. Rubin, Phys. Rev. D **110**, L041303 (2024).
[64] A. Notari, M. Redi, and A. Tesi, J. Cosmol. Astropart. Phys. 11 (2024) 025.
[65] L. Orchard and V. H. Cárdenas, Phys. Dark Universe **46**, 101678 (2024).
[66] A. Hernández-Almada, M. L. Mendoza-Martínez, M. A. García-Aspeitia, and V. Motta, Phys. Dark Universe **46**, 101668 (2024).
[67] M. Malekjani, Z. Davari, and S. Pourojaghi (DESI Collaboration), Phys. Rev. D **111**, 083547 (2025).
[68] W. Giarè, M. Najafi, S. Pan, E. Di Valentino, and J. T. Firouzjaee, J. Cosmol. Astropart. Phys. 10 (2024) 035.
[69] J. Rebouças, D. H. F. de Souza, K. Zhong, V. Miranda, and R. Rosenfeld, J. Cosmol. Astropart. Phys. 02 (2025) 024.
[70] W. Giarè, Phys. Rev. D **112**, 023508 (2025).
[71] C.-G. Park, J. de Cruz Pérez, and B. Ratra, Int. J. Mod. Phys. D **34**, 2550058 (2025).
[72] N. Menci, A. A. Sen, and M. Castellano, Astrophys. J. **976**, 227 (2024).
[73] T.-N. Li, Y.-H. Li, G.-H. Du, P.-J. Wu, L. Feng, J.-F. Zhang, and X. Zhang, Eur. Phys. J. C **85**, 608 (2025).
[74] J.-X. Li and S. Wang, J. Cosmol. Astropart. Phys. 07 (2025) 047.
[75] A. Notari, M. Redi, and A. Tesi, J. Cosmol. Astropart. Phys. 04 (2025) 048.
[76] Q. Gao, Z. Peng, S. Gao, and Y. Gong, Universe **11**, 10 (2025).
[77] R. Fikri, E. ElKhateeb, E. S. Lashin, and W. El Hanafy, Ann. Phys. (Amsterdam) **481**, 170190 (2025).
[78] J.-Q. Jiang, D. Pedrotti, S. S. da Costa, and S. Vagnozzi, Phys. Rev. D **110**, 123519 (2024).
[79] J. Zheng, D.-C. Qiang, and Z.-Q. You, J. Cosmol. Astropart. Phys. 08 (2025) 056.
[80] A. Gómez-Valent and J. Solà Peracaula, Phys. Lett. B **864**, 139391 (2025).
[81] A. Lewis and E. Chamberlain, J. Cosmol. Astropart. Phys. 05 (2025) 065.
[82] W. J. Wolf, C. García-García, and P. G. Ferreira, J. Cosmol. Astropart. Phys. 05 (2025) 034.
[83] A. J. Shajib and J. A. Frieman, Phys. Rev. D **112**, 063508 (2025).
[84] E. Chaussidon *et al.*, Phys. Rev. D **112**, 063548 (2025).
[85] D. A. Kessler, L. A. Escamilla, S. Pan, and E. Di Valentino, arXiv:2504.00776.
[86] Y.-H. Pang, X. Zhang, and Q.-G. Huang, Sci. China Phys. Mech. Astron. **68**, 280410 (2025).
[87] M. Scherer, M. A. Sabogal, R. C. Nunes, and A. De Felice, Phys. Rev. D **112**, 043513 (2025).
[88] E. Specogna, S. A. Adil, E. Ozulker, E. Di Valentino, R. C. Nunes, O. Akarsu, and A. A. Sen, arXiv:2504.17859.
[89] E. M. Teixeira, W. Giarè, N. B. Hogg, T. Montandon, A. Poudou, and V. Poulin, Phys. Rev. D **112**, 023515 (2025).
[90] H. Cheng, E. Di Valentino, L. A. Escamilla, A. A. Sen, and L. Visinelli, J. Cosmol. Astropart. Phys. 09 (2025) 031.
[91] H. Cheng, E. Di Valentino, and L. Visinelli, arXiv:2505.22066.
[92] E. Özülker, E. Di Valentino, and W. Giarè, arXiv:2506.19053.
[93] I. D. Gialamas, G. Hütsi, M. Raidal, J. Urrutia, M. Vasar, and H. Veermäe, Phys. Rev. D **112**, 063551 (2025).
[94] E. Fazzari, W. Giarè, and E. Di Valentino, arXiv:2509.16196.
[95] M. Chevallier and D. Polarski, Int. J. Mod. Phys. D **10**, 213 (2001).
[96] E. V. Linder, Phys. Rev. Lett. **90**, 091301 (2003).
[97] G. Efstathiou, Mon. Not. R. Astron. Soc. **538**, 875 (2025).
[98] G. Ye and S.-J. Lin, arXiv:2505.02207.
[99] L. Verde, T. Treu, and A. G. Riess, Nat. Astron. **3**, 891 (2019).
[100] E. Di Valentino *et al.*, Astropart. Phys. **131**, 102605 (2021).
[101] E. Di Valentino, O. Mena, S. Pan, L. Visinelli, W. Yang, A. Melchiorri, D. F. Mota, A. G. Riess, and J. Silk, Classical Quantum Gravity **38**, 153001 (2021).
[102] L. Perivolaropoulos and F. Skara, New Astron. Rev. **95**, 101659 (2022).
[103] N. Schöneberg, G. Franco Abellán, A. Pérez Sánchez, S. J. Witte, V. Poulin, and J. Lesgourgues, Phys. Rep. **984**, 1 (2022).
[104] P. Shah, P. Lemos, and O. Lahav, Astron. Astrophys. Rev. **29**, 9 (2021).
[105] E. Abdalla *et al.*, J. High Energy Astrophys. **34**, 49 (2022).
[106] E. Di Valentino, Universe **8**, 399 (2022).
[107] M. Kamionkowski and A. G. Riess, Annu. Rev. Nucl. Part. Sci. **73**, 153 (2023).
[108] W. Giarè, *The Hubble Constant Tension* (Springer, Singapore, 2024).
[109] J.-P. Hu and F.-Y. Wang, Universe **9**, 94 (2023).
[110] L. Verde, N. Schöneberg, and H. Gil-Marín, Annu. Rev. Astron. Astrophys. **62**, 287 (2024).
[111] *The Hubble Constant Tension*, edited by E. Di Valentino and D. Brout, Springer Series in Astrophysics and Cosmology (Springer, New York, 2024).
[112] L. Perivolaropoulos, Phys. Rev. D **110**, 123518 (2024).
[113] E. Di Valentino *et al.* (CosmoVerse Collaboration), Phys. Dark Universe **49**, 101965 (2025).
[114] I. J. Allali, A. Notari, and F. Rompineve, J. Cosmol. Astropart. Phys. 03 (2025) 023.

[115] W. Giarè, M. A. Sabogal, R. C. Nunes, and E. Di Valentino, Phys. Rev. Lett. **133**, 251003 (2024).
[116] H. Wang, G. Ye, J.-Q. Jiang, and Y.-S. Piao, Phys. Rev. D **111**, 123505 (2025).
[117] V. Poulin, T. L. Smith, R. Calderón, and T. Simon, arXiv:2505.08051.
[118] A. Cuoco, J. Lesgourgues, G. Mangano, and S. Pastor, Phys. Rev. D **71**, 123501 (2005).
[119] Y. Farzan and S. Hannestad, J. Cosmol. Astropart. Phys. 02 (2016) 058.
[120] G. Dvali and L. Funcke, Phys. Rev. D **93**, 113002 (2016).
[121] N. Bellomo, E. Bellini, B. Hu, R. Jimenez, C. Pena-Garay, and L. Verde, J. Cosmol. Astropart. Phys. 02 (2017) 043.
[122] M. Lattanzi and M. Gerbino, Front. Phys. **5**, 70 (2018).
[123] C. S. Lorenz, L. Funcke, E. Calabrese, and S. Hannestad, Phys. Rev. D **99**, 023501 (2019).
[124] C. D. Kreisch, F.-Y. Cyr-Racine, and O. Doré, Phys. Rev. D **101**, 123505 (2020).
[125] I. M. Oldengott, G. Barenboim, S. Kahlen, J. Salvado, and D. J. Schwarz, J. Cosmol. Astropart. Phys. 04 (2019) 049.
[126] Z. Chacko, A. Dev, P. Du, V. Poulin, and Y. Tsai, J. High Energy Phys. 04 (2020) 020.
[127] S. Roy Choudhury and S. Choubey, J. Cosmol. Astropart. Phys. 09 (2018) 017.
[128] S. Roy Choudhury and A. Naskar, Eur. Phys. J. C **79**, 262 (2019).
[129] S. Roy Choudhury and S. Hannestad, J. Cosmol. Astropart. Phys. 07 (2020) 037.
[130] Z. Chacko, A. Dev, P. Du, V. Poulin, and Y. Tsai, Phys. Rev. D **103**, 043519 (2021).
[131] M. Escudero, J. Lopez-Pavon, N. Rius, and S. Sandner, J. High Energy Phys. 12 (2020) 119.
[132] I. Esteban and J. Salvado, J. Cosmol. Astropart. Phys. 05 (2021) 036.
[133] I. Esteban, O. Mena, and J. Salvado, Phys. Rev. D **106**, 083516 (2022).
[134] G. Franco Abellán, Z. Chacko, A. Dev, P. Du, V. Poulin, and Y. Tsai, J. High Energy Phys. 08 (2022) 076.
[135] G. Dvali, L. Funcke, and T. Vachaspati, Phys. Rev. Lett. **130**, 091601 (2023).
[136] J. Alvey, M. Escudero, N. Sabti, and T. Schwetz, Phys. Rev. D **105**, 063501 (2022).
[137] J. Alvey, M. Escudero, and N. Sabti, J. Cosmol. Astropart. Phys. 02 (2022) 037.
[138] C. S. Lorenz, L. Funcke, M. Löffler, and E. Calabrese, Phys. Rev. D **104**, 123518 (2021).
[139] F. D'Eramo, E. Di Valentino, W. Giarè, F. Hajkarim, A. Melchiorri, O. Mena, F. Renzi, and S. Yun, J. Cosmol. Astropart. Phys. 09 (2022) 022.
[140] M. Escudero, T. Schwetz, and J. Terol-Calvo, J. High Energy Phys. 02 (2023) 142; 06 (2024) 119(A).
[141] M. Sen and A. Y. Smirnov, J. Cosmol. Astropart. Phys. 01 (2024) 040.
[142] W. Giarè, A. Gómez-Valent, E. Di Valentino, and C. van de Bruck, Phys. Rev. D **109**, 063516 (2024).
[143] P. Brax, C. van de Bruck, E. Di Valentino, W. Giarè, and S. Trojanowski, Mon. Not. R. Astron. Soc. **527**, L122 (2023).
[144] P. Brax, C. van de Bruck, E. Di Valentino, W. Giarè, and S. Trojanowski, Phys. Dark Universe **42**, 101321 (2023).
[145] I. J. Allali, D. Aloni, and N. Schöneberg, J. Cosmol. Astropart. Phys. 09 (2024) 019.
[146] S. Trojanowski and L. Zu, arXiv:2505.20396.
[147] C. Benso, T. Schwetz, and D. Vatsyayan, J. Cosmol. Astropart. Phys. 04 (2025) 054.
[148] L. Zu, W. Giarè, C. Zhang, E. Di Valentino, Y.-L. S. Tsai, and S. Trojanowski, arXiv:2501.13785.
[149] A. Poudou, T. Simon, T. Montandon, E. M. Teixeira, and V. Poulin, arXiv:2503.10485.
[150] A. Das, P. S. B. Dev, C. Gao, S. Ghosh, and T. Kim, arXiv:2506.08085.
[151] E. V. Linder, Phys. Rev. D **72**, 043529 (2005).
[152] E. V. Linder and R. N. Cahn, Astropart. Phys. **28**, 481 (2007).
[153] E. V. Linder, Astropart. Phys. **86**, 41 (2017).
[154] G. R. Dvali, G. Gabadadze, and M. Porrati, Phys. Lett. B **485**, 208 (2000).
[155] C.-P. Ma and E. Bertschinger, Astrophys. J. **455**, 7 (1995).
[156] F. Bernardeau, S. Colombi, E. Gaztanaga, and R. Scoccimarro, Phys. Rep. **367**, 1 (2002).
[157] L.-M. Wang and P. J. Steinhardt, Astrophys. J. **508**, 483 (1998).
[158] S. Tsujikawa, R. Gannouji, B. Moraes, and D. Polarski, Phys. Rev. D **80**, 084044 (2009).
[159] R. Gannouji, B. Moraes, and D. Polarski, J. Cosmol. Astropart. Phys. 02 (2009) 034.
[160] N.-M. Nguyen, D. Huterer, and Y. Wen, Phys. Rev. Lett. **131**, 111001 (2023).
[161] E. Specogna, E. Di Valentino, J. L. Said, and N.-M. Nguyen, Phys. Rev. D **109**, 043528 (2024).
[162] A. Kiakotou, O. Elgaroy, and O. Lahav, Phys. Rev. D **77**, 063005 (2008).
[163] W. Giarè, O. Mena, and E. Di Valentino, Phys. Rev. D **108**, 103539 (2023).
[164] E. Di Valentino, S. Gariazzo, W. Giarè, and O. Mena, Phys. Rev. D **108**, 083509 (2023).
[165] A. Lewis and A. Challinor, Phys. Rep. **429**, 1 (2006).
[166] M. Kaplinghat, L. Knox, and Y.-S. Song, Phys. Rev. Lett. **91**, 241301 (2003).
[167] J. Lesgourgues, L. Perotto, S. Pastor, and M. Piat, Phys. Rev. D **73**, 045021 (2006).
[168] A. Lewis, A. Challinor, and A. Lasenby, Astrophys. J. **538**, 473 (2000).
[169] C. Howlett, A. Lewis, A. Hall, and A. Challinor, J. Cosmol. Astropart. Phys. 04 (2012) 027.
[170] J. Torrado and A. Lewis, J. Cosmol. Astropart. Phys. 05 (2021) 057.
[171] A. Lewis, J. Cosmol. Astropart. Phys. 08 (2025) 025.
[172] N. Aghanim *et al.* (Planck Collaboration), Astron. Astrophys. **641**, A5 (2020).
[173] Y. Akrami *et al.* (Planck Collaboration), Astron. Astrophys. **641**, A4 (2020).
[174] N. Aghanim *et al.* (Planck Collaboration), Astron. Astrophys. **641**, A8 (2020).
[175] E. Rosenberg, S. Gratton, and G. Efstathiou, Mon. Not. R. Astron. Soc. **517**, 4620 (2022).
[176] Y. Akrami *et al.* (Planck Collaboration), Astron. Astrophys. **643**, A42 (2020).
[177] J. Carron, M. Mirmelstein, and A. Lewis, J. Cosmol. Astropart. Phys. 09 (2022) 039.

[178] E. Calabrese, A. Slosar, A. Melchiorri, G. F. Smoot, and O. Zahn, Phys. Rev. D **77**, 123531 (2008).
[179] E. Di Valentino, A. Melchiorri, and J. Silk, Phys. Rev. D **93**, 023513 (2016).
[180] F. Renzi, E. Di Valentino, and A. Melchiorri, Phys. Rev. D **97**, 123534 (2018).
[181] G. Domènech, X. Chen, M. Kamionkowski, and A. Loeb, J. Cosmol. Astropart. Phys. 10 (2020) 005.
[182] E. Di Valentino, S. Galli, M. Lattanzi, A. Melchiorri, P. Natoli, L. Pagano, and N. Said, Phys. Rev. D **88**, 023501 (2013).
[183] F. Capozzi, E. Di Valentino, E. Lisi, A. Marrone, A. Melchiorri, and A. Palazzo, Phys. Rev. D **95**, 096014 (2017); **101**, 116013(A) (2020).
[184] E. Di Valentino and A. Melchiorri, Astrophys. J. Lett. **931**, L18 (2022).
[185] F. Capozzi, E. Di Valentino, E. Lisi, A. Marrone, A. Melchiorri, and A. Palazzo, Phys. Rev. D **104**, 083031 (2021).
[186] I. J. Allali and A. Notari, J. Cosmol. Astropart. Phys. 12 (2024) 020.
[187] E. Specogna, W. Giarè, and E. Di Valentino, Phys. Rev. D **111**, 103510 (2025).
[188] M. Ishak *et al.*, J. Cosmol. Astropart. Phys. 09 (2025) 053.
[189] A. G. Adame *et al.* (DESI Collaboration), J. Cosmol. Astropart. Phys. 07 (2025) 028.
[190] U. Andrade *et al.* (DESI Collaboration), Phys. Rev. D **112**, 083512 (2025).
[191] M. Abdul Karim *et al.* (DESI Collaboration), Phys. Rev. D **112**, 083514 (2025).
[192] D. Brout *et al.*, Astrophys. J. **938**, 110 (2022).
[193] T. M. C. Abbott *et al.* (DES Collaboration), Astrophys. J. Lett. **973**, L14 (2024).
[194] B. O. Sánchez *et al.* (DES Collaboration), Astrophys. J. **975**, 5 (2024).
[195] M. Vincenzi *et al.* (DES Collaboration), Astrophys. J. **975**, 86 (2024).
[196] D. Rubin *et al.*, arXiv:2311.12098.
[197] M. Vincenzi *et al.* (DES Collaboration), Mon. Not. R. Astron. Soc. **541**, 2585 (2025).
[198] E. Di Valentino *et al.*, Astropart. Phys. **131**, 102604 (2021).
[199] E. Di Valentino and S. Bridle, Symmetry **10**, 585 (2018).
[200] R. C. Nunes and S. Vagnozzi, Mon. Not. R. Astron. Soc. **505**, 5427 (2021).
[201] A. Amon *et al.* (DES Collaboration), Phys. Rev. D **105**, 023514 (2022).
[202] L. F. Secco *et al.* (DES Collaboration), Phys. Rev. D **105**, 023515 (2022).
[203] M. Asgari *et al.* (KiDS Collaboration), Astron. Astrophys. **645**, A104 (2021).
[204] M. Asgari *et al.*, Astron. Astrophys. **634**, A127 (2020).
[205] S. Joudaki *et al.*, Astron. Astrophys. **638**, L1 (2020).
[206] G. D'Amico, J. Gleyzes, N. Kokron, K. Markovic, L. Senatore, P. Zhang, F. Beutler, and H. Gil-Marín, J. Cosmol. Astropart. Phys. 05 (2020) 005.
[207] T. M. C. Abbott *et al.* (Kilo-Degree Survey, DES Collaborations), Open J. Astrophys. **6**, 2305.17173 (2023).
[208] T. Tröster *et al.*, Astron. Astrophys. **633**, L10 (2020).
[209] C. Heymans *et al.*, Astron. Astrophys. **646**, A140 (2021).
[210] R. Dalal *et al.*, Phys. Rev. D **108**, 123519 (2023).
[211] S. Chen *et al.*, Phys. Rev. D **110**, 103518 (2024).
[212] J. Kim *et al.*, J. Cosmol. Astropart. Phys. 12 (2024) 022.
[213] L. Faga *et al.* (DES Collaboration), Mon. Not. R. Astron. Soc. **536**, 1586 (2024).
[214] J. Harnois-Deraps *et al.*, Mon. Not. R. Astron. Soc. **534**, 3305 (2024).
[215] A. Dvornik *et al.*, Astron. Astrophys. **675**, A189 (2023); **688**, C3(E) (2024).
[216] T. M. C. Abbott *et al.* (DES Collaboration), Phys. Rev. D **105**, 023520 (2022).
[217] A. H. Wright *et al.*, arXiv:2503.19441.
[218] B. Stölzner *et al.*, Astron. Astrophys. **702**, A169 (2025).